OBSERVATIONS ON LAND-SNAIL SHELLS IN NEAR-ULTRAVIOLET, VISIBLE AND NEAR-INFRARED RADIATION

ENRICO SAVAZZI[1] AND TAKENORI SASAKI[2]

[1]*School of Geosciences, Monash University, Building 28, Victoria 3800, Australia; and*
[2]*The University Museum, The University of Tokyo, 7-3-1 Hongo, Bunkyo-ku, Tokyo 113-0033, Japan*

Correspondence: Enrico Savazzi, Hagelgränd 8, 75646 Uppsala, Sweden; e-mail: enrico8@savazzi.net

(Received 18 March 2013; accepted 28 November 2012)

ABSTRACT

The shells of a broad range of land snails were digitally imaged in the near-ultraviolet (NUV), visible range (VIS) and near infrared (NIR). NIR images were recorded in both incident and transmitted illumination. In most cases, shell and periostracal pigmentation observed in the VIS was completely translucent in the NIR, while its contrast was enhanced in the NUV. Exceptions to the above rule fit into four main categories. (1) Snails with green or tan shells or periostraca, presumably functional as camouflage among vegetation, were often highly absorbing in the NUV, thus matching the optical characteristics of green vegetation in this range. (2) Pigmented spiral stripes in the shells of several Camaenidae and Helicidae were adjacent to nonpigmented areas that display a heightened reflectivity and reduced translucence in the VIS and NIR. This enhanced the contrast of the colour pattern in the VIS, but appeared to lack functions in the NIR. (3) Snails from arid or desert environments exposed to high levels of sunlight often have largely white shells, highly reflective throughout the studied range of wavelengths. This is likely an adaptation to reduce the thermal effects of solar irradiation, and may also be a form of masquerading camouflage. (4) Among numerous Bradybaenidae and a few Camaenidae, Helicidae, Orthalicidae and Enidae, reflective patches or stripes, white in the VIS, were present in the periostracum or outermost shell layer. These structures were highly reflective (and highly opaque to transmitted radiation) across the NUV, VIS and NIR. They may have a dual function as disruptive camouflage in the NUV and VIS, and as reflectors to reduce the thermal effects of solar irradiation in the VIS and NIR.

INTRODUCTION

In most species of land snails, shells are frequently exposed to direct or indirect sunlight, which contains substantial amounts of near-ultraviolet and near-infrared radiation, in addition to visible light. Numerous terrestrial organisms are known to see in the visible and ultraviolet ranges (see Discussion section), including snail predators as well as the snail themselves. Solar radiation in the visible and infrared ranges contributes to the heating of snail shells and contained tissues (see Discussion section). Thus, it is to be expected that the appearance of land snail shells at these wavelengths could be related to functional or adaptive features in contexts such as predator avoidance, intraspecific recognition and temperature regulation. However, literature on the appearance of land snail shells (or, more generally, mollusc shells) imaged in the near ultraviolet and near infrared appears to be absent.

In biology, near-ultraviolet imaging of macroscopical features is used mainly to study nectar tracks in flowers (in connection with UV vision by pollinating organisms, Primack, 1982; Biedinger & Barthlott, 1993), the plumage of birds (mainly in the context of UV vision and mate selection by these organisms, e.g. Andersson & Amundsen, 1997; Bennett, Cuthill & Partridge, 1997; Hunt *et al.*, 1997; Ödeen, Håstad & Alström, 2011) and lepidopteran wings (in connection with UV vision, intraspecific recognition and predation, e.g. Imafuku, Hirose & Takeuchi, 2002; Lyytinen, Lindström & Mappes, 2004; Heppner, 2008). Near-infrared imaging of macroscopic biological features is commonly used in the remote sensing of vegetation (Campbell, 2002), but infrequently for other macroscopic organisms. The literature on near-ultraviolet and near-infrared imaging in science, medicine, forensics and conservation was summarized by Savazzi (2011).

Studies on ultraviolet-induced shell fluorescence in the visible range (e.g. Woodbridge, 1961) are not relevant to imaging in the ultraviolet range, because light absorption at one wavelength does not necessarily result in fluorescent emission at a different wavelength, and both the absorbed and

emitted wavelengths are highly material-specific. The present study does not specifically examine fluorescence. Because we used an illumination source with a broad wavelength spectrum similar to daylight, any fluorescent emission in this spectrum is combined with the effects of direct illumination.

The visible portion of the electromagnetic spectrum extends approximately between the wavelengths of 400 and 700 nm, or, including wavelengths that are only faintly perceived by the human eye, 390 to 750 nm (e.g. Starr, 2005; King, 2005). The ultraviolet range is adjacent to the blue/indigo portion of the visible spectrum, and consists of shorter wavelengths. The infrared is adjacent to the red portion of the visible spectrum, and consists of longer wavelengths. The sensitivity of human photopigments decreases gradually, rather than abruptly, at the borders of the visible range, and the transparency of the lens and internal medium of the human eye decreases sharply in the ultraviolet (King, 2005; Starr, 2005). Modest individual differences in spectral perception are documented in humans (e.g. Jameson, Highnote & Wasserman, 2001). For practical purposes, both ultraviolet and infrared radiation can be regarded as invisible (disregarding any fluorescence in the visible range of the subject or of parts of the eyes induced by ultraviolet radiation).

The wavelength range of electromagnetic radiation used for imaging in the present study extends from c. 340 to 1,000 nm (see the Methods section), and includes the near-ultraviolet (more specifically, a major portion of the UV-A range), henceforth abbreviated as NUV (340–400 nm), and near-infrared, henceforth abbreviated as NIR (700–1,000 nm). In the literature (e.g. Shaw et al., 2009) the wavelength ranges included in the NUV and NIR are somewhat variable and no standard definition of these terms exists. Visible light, and images showing the appearance in this wavelength range, are herein abbreviated as VIS (an informal abbreviation broadly used together with NUV and NIR).

The colours of mollusc shells result from a variety of causes, including light absorption, fluorescence, translucence, diffusion, diffraction and refraction by chemical pigments as well as structural materials (see, e.g. Comfort, 1951; Hedegaard, Bardeau & Chateigner, 2006). A detailed survey of these and other causes of colour in a broad variety of materials can be found in Tilley (2011). The present paper does not investigate the physical or chemical causes of the observed colour patterns.

This study recorded the appearance of land snail shells in the NUV, VIS and NIR with a modified digital camera, and discussed some of the possible adaptive values of the observed features. The results of our observations were categorized according to whether the observed colour originates from the periostracum or underlying shell (or a combination of both). Periostracal colour patterns were easily detected by removing portions of periostracum, e.g. by scraping with a blade, and comparing the observed features. Colour embedded in the outermost shell layers (henceforth referred to as shell colour) was not removed with the periostracum and often became clearer after this treatment. We did not examine the colour of periostracum alone, isolated from the shell. We cannot exclude that an isolated periostracum would display optical properties different from those observed in the same periostracum attached to the shell.

MATERIAL AND METHODS

Specimens

Specimens illustrated in this paper are deposited in the collections of the University Museum, Tokyo University, Japan, except as noted in the figure captions. The majority of the specimens were not collected by us. A portion of the specimens came from museum collections, and others were obtained from private collectors. As a result, the length and conditions of storage after collection, as well as the methods used to remove the soft parts, varied considerably and were often not documented. We excluded from this study any specimens that displayed obvious signs of having been collected as empty shells of naturally dead individuals.

The present study dealt exclusively with shell specimens in dry collections, and examined a broad range of species of land snails, chosen for their availability to the authors and for their varied appearance in VIS (and thus, potentially varied appearance in NUV and NIR). However, this was not meant to be a comprehensive survey of land snails, either in a taxonomic sense or as an exhaustive survey of types of colour patterns. Imaging was carried out on whole shells with periostraca in their natural state, including specimens that partly or totally lack periostraca, when the collection materials and literature suggest that this is the normal life condition for the species. The living versus empty-shell state of specimens, the method used for killing the specimens, the duration of specimen storage in collection, the type of storage containers and the dry versus wet state of empty shells did not significantly affect their NUV, VIS and NIR images.

Illumination types

The illustrations of this paper required incident illumination of the specimens to assess the reflective optical qualities of the periostracum and underlying shell, as well as a form of transmitted illumination to assess the behaviour of translucent structures in the shell and periostracum. The physical arrangement of incident illumination used for the illustrations of this paper conformed to the standard incident illumination used in the photographic documentation of opaque three-dimensional specimens, and consisted of a single, moderately diffused light source positioned at the top left of the specimen, with reflectors placed along the bottom and right side of the subject to fill the shadows.

A highly diffused type of transmitted illumination was achieved by surrounding the portion of the subject facing toward the camera with a blackened metal tube. This caused the subject to be directly illuminated only on its portions facing away from the camera. Only radiation transmitted and diffused through the specimen and emerging from its topmost surfaces was recorded in these images. This type of illumination can also be described as dark-field, since light reaches the subject from an off-axis source at the rear of the subject and outside the field of view. A problem with this type of transmitted illumination is that it is difficult to completely shield the camera-facing portion of the subject from incident illumination, often resulting in a brightly illuminated perimeter of the subject.

Either incident or transmitted illumination (as specified in the figure captions) was used for imaging in the NIR, because of the higher translucence in this range of most of the studied shells. Shell translucence proved too low for adequate transmitted illumination in VIS and NUV. Therefore, NUV and VIS images in the illustrations of this paper were exclusively recorded with incident illumination.

Photographic equipment and techniques

The large majority of digital cameras, lenses, light sources, diffusers and reflectors designed for photography in VIS are unsuitable for NUV photography. In addition, without attention to specific technical pitfalls, digital NUV photography is very likely to produce unusable or misleading results. Photography

in the NIR is sometimes feasible with ordinary, unmodified digital cameras and accessories, albeit at the price of very long exposure times and, consequently, noisy images.

The rest of this section contains brief descriptions of the principal pieces of photographic equipment used for NUV and NIR photography in this study. A more detailed discussion of the equipment and techniques for digital NUV and NIR photography has been given by Savazzi (2011). Some additional information is also available (e.g. Verhoeven, 2008; Verhoeven & Schmitt, 2008; Rutowski & Macedonia, 2008; Verhoeven *et al*., 2009). The principal goal of the equipment and techniques described below is to allow the recording of separate images in NUV, VIS and NIR without altering the reciprocal positions of camera, subject and illumination, and without changing lens aperture and focus.

Camera: Nikon D70s DSLR (digital single-lens reflex), modified by replacing the anti-aliasing, UV-blocking and IR-blocking filter (originally mounted in front of the sensor package) with a silica-glass optical window marketed for this purpose by LifePixel, Inc. (Mukilteo, Washington, USA) (http://www.lifepixel.com). This modification does not replace the glass window that is an integral part of the sensor chip package.

This modification was found to enhance the sensitivity of this camera model to 700 nm radiation (i.e. in the deep visible red, close to the border with NIR) by a factor of 20 (data at http://astrosurf.com/buil/d70/ircut.htm). Sensitivity in the NIR range was enhanced to a much greater extent. NUV sensitivity was enhanced to a much lesser degree than in the NIR. However, because of the higher energy carried by NUV radiation (relative to VIS and NIR radiation), NUV images are remarkably noise-free. In practice, the first author found the modified camera to provide useful imaging capabilities in a spectral range between 340 and 1,000 nm. This spectral range was verified by imaging a series of monochromatic LEDs emitting known wavelengths. These devices are cheap, stable and narrow-band sources of radiation.

NUV-pass filter: For this study, we used a U filter (Baader Planetarium, Mammendorf, Germany) (http://www.baader-planetarium.com), with highest transmission at *c*. 350 or 360 nm (the data vary among information sources, e.g. http://www.astrosurf.org/pellier/comparuvfilters). The reasons for choosing this filter have been explained by Savazzi (2011: 482).

VIS-pass filter: The B + W 486 filter is designed to reject both NUV and NIR radiation, and to transmit only VIS. By setting a suitable custom white balance in the camera settings, with this filter it is possible to approximately restore the original spectral response of the camera prior to modification. This filter was used to take images in the VIS.

NIR-pass filters: For NIR imaging, an unbranded filter with 50% cut-off at a wavelength of 800 nm was used. Filters with cut-offs at wavelengths of 750, 900 and 1,000 nm were also tested with the subjects of this study, but were not found to provide sufficiently different information to justify their use. The 800 nm filter proved to be a good compromise, because lower cut-off wavelengths result in the recording of noticeable amounts of visible red light, and higher ones yield a low illumination level and cause noisier images.

Neutral density (ND) filters: The response curve of the unfiltered camera sensor is highly nonlinear with respect to wavelength, and from a maximum at *c*. 800 nm decreases sharply throughout the VIS and NUV ranges, requiring an adjustment of 10–12 stops (i.e. a factor of more than 10^3) when imaging at different wavelengths. This was compensated by stacking ND filters of appropriate strengths together with the above filters. A Hoya NDX400 (with attenuation factor of 400) was used in the VIS, stacked onto the B + W 486. A B + W ND 3.0 (with attenuation factor of 10^3) was used in the NIR, stacked onto the 800 nm filter. These combinations of filters allowed the imaging of the same subject at different wavelengths with only modest adjustments in illumination intensity (1–2 stops) and without changes in lens aperture or distance between illuminator and subject, making the visual comparison of images easier.

Lens: A Rodenstock UV Rodagon 60 mm f/5.6 lens (currently discontinued) was used for most photographic documentation for this study. This lens was designed for microfilm reproduction with UV illumination. This and very few other lens models allow the digital imaging from the NUV to the NIR ranges without refocusing (see discussion by Savazzi, 2011).

Light sources: A Gemini 500 R studio electronic flash (Bowens, Clacton-on-Sea, UK) (http://www.bowens.co.uk) was used as light source for almost all images of this study. The original xenon tube has a UV-absorbing coating and was replaced with a similar but uncoated tube, separately available from the same manufacturer. The uncoated tube, as tested by the first author, emits approximately three times the amount of NUV produced by the original tube. In spite of this, NUV imaging for this study often required the use of the flash unit at full power (500 W/s) and close range (20–25 cm from the subject). This model was chosen for the present purpose, because it is currently the most powerful Bowens self-contained unit that does not use forced cooling by internal fans (which generate air currents that may move small subjects at close distances).

A 40-W incandescent light bulb in a hand-held fixture was used as an alternative, easily transported source of VIS and NIR radiation while visiting museum collections. This light source emits plentiful NIR radiation, but of course does not allow NUV imaging. Patterned aluminium panels originally designed for use in lighting fixtures were used as reflectors, since commonly used photographic reflectors tend to perform poorly in the NUV and/or NIR.

Illustration techniques

The simplest way to display NUV and NIR images for illustration purposes is to convert them to greyscale. Although the recorded images, in their original format, do contain colour information, this is largely an artefact due to the way sensors designed to record red, green and blue light react to wavelengths outside the VIS range. Both NIR and NUV images, as originally recorded, display a predominant colour cast (usually pink, red or indigo) that is generally perceived as unpleasant and should be removed. These images were converted to greyscale by lowering their colour saturation to zero in an image editor (Adobe Photoshop CS5 and CS6). This operation effectively removed all colour information. Images recorded in VIS were converted to greyscale with the default Photoshop settings of the 'Black & White' adjustment tool (40% red, 60% yellow, 40% green, 60% cyan, 20% blue and 80% magenta).

Contrast, luminance and/or gamma of images were also adjusted to provide a visually satisfactory image. While NUV and VIS images generally needed little or no adjustment, incident NIR images and, to a lesser extent, transmitted NIR images often required a substantial increase in contrast and, sometimes, the application of a nonlinear transfer curve (with the Curves functionality provided by Adobe Photoshop CS5).

This results in an enhanced noise level of NIR images, which fortunately is not very noticeable once their size is reduced for publication.

One of the purposes of displaying NIR and NUV images in the present paper is to visually compare them with images recorded in VIS. The latter images could, in principle, be displayed in colour. However, our initial attempts to do so showed that it is difficult to visually compare greyscale images with colour ones. This is compounded by the fact, well known to photographers, that the human perception of colour is easily influenced by the quality of illumination and other characteristics of the surrounding environment. Thus, most illustrations of this paper are greyscale images.

One colour figure (Fig. 1) provides a selection of particularly interesting images recorded in VIS, as well as false-colour composites. It proved useful to create false-colour composites of images recorded in incident NUV (remapped as blue in the images) and transmitted NIR (remapped as red). Intense blue areas corresponded to a predominant high NUV reflectivity and intense red to a predominant high NIR transmission. Magenta areas corresponded to a mixture of reflected NUV and transmitted NIR. Examples of this technique are shown in Figure 1B, D, K, N and P. The peripheral shell areas in these composite images displayed a red tinge (especially in early whorls), caused by diffused NIR radiation. A similar technique was used to produce composite images of incident NIR (remapped as green) and transmitted NIR (remapped as red) (Fig. 1L, O). Yellow/orange areas in these images corresponded to a combination of high levels of both reflected and transmitted NIR, and green areas to prevalent reflected NIR. A combination of high transmitted NIR and low reflected NIR should be displayed as red, but such areas are absent in these composite images.

Terminology

The terms used in this paper to qualitatively describe the optical behaviour of shell and periostracum in NUV and NIR images correspond to common terms used in visible light, e.g. dark versus light to characterize a low versus high amount of re-emission of radiation, and translucent versus opaque to describe the proportion of transmitted radiation. Reflection (usually diffuse and in the sense of back-scattering, rather than specular) is involved in these properties. Specifically, a high reflectivity results in a light appearance in incident illumination, as well as in high opacity, and thus rendering as dark, in transmitted illumination.

RESULTS

General appearance in NUV and NIR

In most cases, the NUV appearance of shell colour patterns was comparable in appearance with that in VIS. The coloured areas were virtually identical in placement and size in both wavelength ranges. However, NUV images typically display radiation-absorbing areas as darker than in VIS and noncoloured (i.e. background) areas as more reflective and less translucent, and consequently lighter than in VIS. In general, VIS images tended to appear faded or 'washed out', compared with NUV images. In the NIR, on the other hand, almost all shell colour was undetectable or very low in contrast. Imaging in this range typically displayed a very light shell, a complete or almost complete lack of spatially uneven absorbing areas and overall a more translucent shell than in VIS. Examples of this behaviour are shown in Figure 2A–H.

In most species of land snails, repaired shell damage was the only feature that stood out with a darker tone from the rest of the shell in NIR images, probably as a result of the embedding of mineral grains from the substrate in the scar structure. This was also the case with mineral grains trapped among fine periostracal relief (Fig. 2E).

NIR reflection and absorption by shells

Liguus virgineus (Orthalicidae) conformed to the general pattern of high contrast of the pigmented spiral lines in incident NUV and VIS, and very low contrast in incident NIR illumination (Fig. 2F–H). Additionally, spiral bands of shell material adjacent to pigmented stripes were more opaque, and therefore darker, than the rest of the shell in transmitted NIR (Fig. 2I). As a result, the areas occupied by pigmented stripes stood out in a lighter tone than surrounding areas in transmitted NIR, thus yielding a 'negative' image of the VIS colour pattern. Incident NIR images of this species (which largely remove the colour pattern) showed a fine shell relief, especially in grazing illumination, i.e. the colour bands corresponded to very shallow furrows in the shell surface (Fig. 2H). Thus, the NIR-opaque areas adjacent to colour bands represented regions of increased shell thickness. The additional thickness, and possibly a different shell structure, caused a moderate increase in shell reflectivity (and opacity to transmitted illumination) in VIS, which in turn increased the whiteness of the shell surfaces adjacent to pigmented bands and, as a result, the contrast of the colour pattern in VIS. It is possible that a comparable effect also takes place in the NUV, albeit the higher shell opacity to NUV makes this effect much less noticeable.

A comparable, lower translucence of areas neighbouring VIS colour patterns was also observed in representatives of the Camaenidae, albeit not accompanied by a detectable surface relief (Fig. 2J–M). This also resulted in an apparent inversion of the colour pattern in incident VIS versus transmitted NIR images (Fig. 2K and M, respectively). A similar phenomenon was also observed in the spiral bands of the helicid *Otala lactea* (Fig. 2N–O). In Figure 2M, the inner surface, as seen through the shell aperture, was mainly illuminated by incident NIR transmitted and diffused through other shell regions, and therefore did not display an inverted pattern relative to VIS. Note also that the base of the whorl in Figure 2M differed from the inverted pattern displayed by other regions of the whorl in displaying no NIR-absorbing colour, thus proving that the complementarity of the incident VIS and transmitted NIR patterns is not an 'obligatory' property across the whole shell. False-colour composite images obtained with the procedure described in the Methods section were useful to show the inverse relationship between reflectivity in incident NUV and absorption in transmitted NIR (remapped as blue and red, respectively, in Fig. 1B, D).

Exceptions to the high translucence of shell pigments in the NIR were found among the New Zealand Rhytididae (Fig. 3A–D). The shells of several species were dark and displayed collabral or spiral bands of dark brown, black and/or dark greenish colours in the VIS. In representatives of this family the colour patterns were still visible, albeit lower in contrast, in incident NIR images (Fig. 3B, D). It is interesting to note that some of the spiral lines detectable in VIS (specifically, reddish brown ones) were absent in NIR images, while dark green or black lines in VIS range were also displayed in incident NIR. Specimens of this family were not available for NUV imaging. The caryodid *Pedinogyra hayii* from Australia was superficially similar to these Rhytididae in shell colour in VIS, shell geometry and size, but its shell colour was completely undetectable in both incident and transmitted NIR.

A few tree snails in the families Bradybaenidae and Camaenidae displayed a green colour of the outer shell layer (Figs 1G–H, 4A–H). Unlike the Rhytididae, this colour did
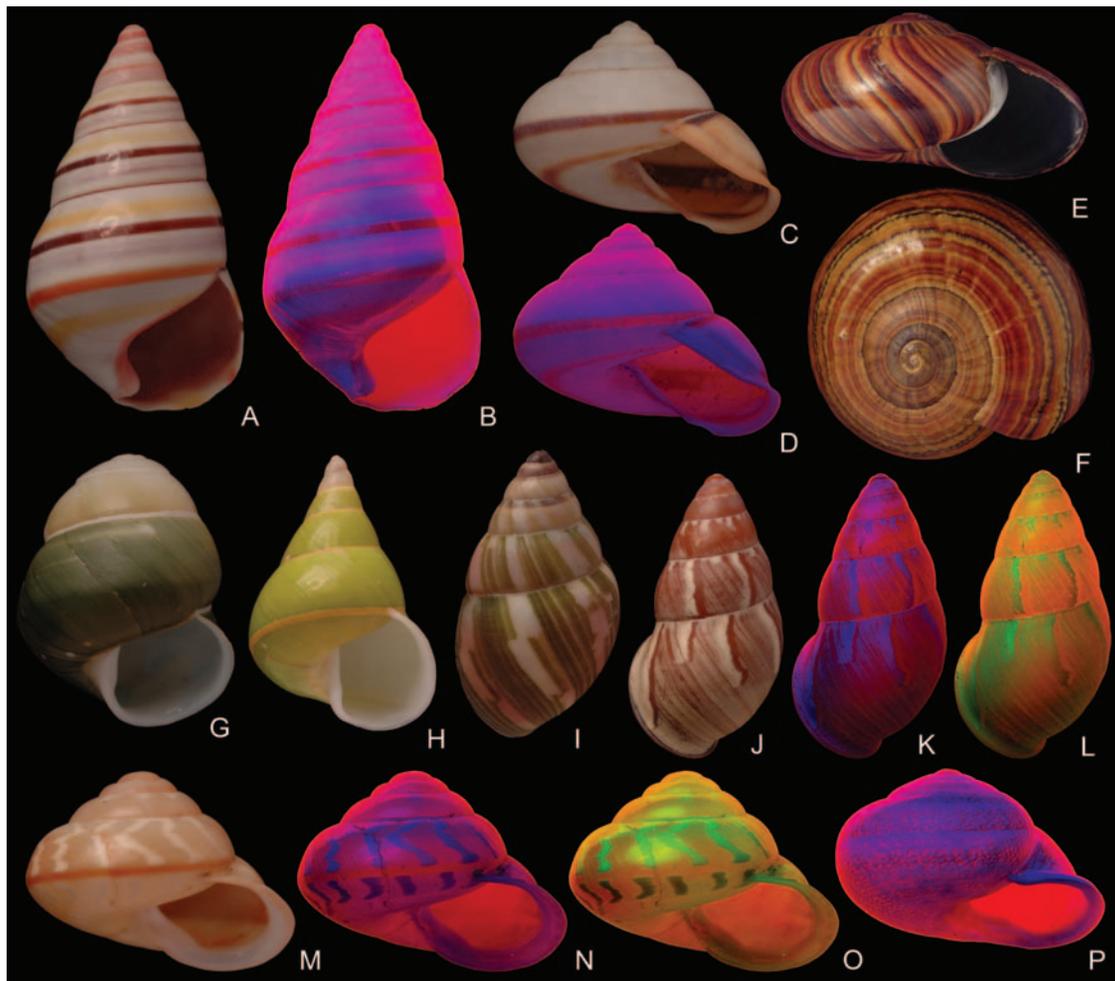
Figure 1. A, B. *Liguus virgineus* (Linnaeus, 1758), Dominican Republic, VIS (**A**) and composite of NUV and transmitted NIR (**B**). **C, D.** *Papuina gamelia* (Angas, 1867), VIS (**C**) and composite of NUV and transmitted NIR (**D**). **E.** *Paryphanta lignaria* (Hutton, 1880), South Island, New Zealand, VIS. **F.** *Paryphanta* (or *Powelliphanta*) *hochstetteri anatokiensis* (Powell, 1938), central Southern Alps, New Zealand, VIS. **G.** *Helicostyla florida* (Sowerby, 1841), Mindoro Island, Philippines, VIS. **H.** *Papustyla pulcherrima* Rensch, 1931, Manus I., Papua New Guinea, VIS. **I.** *Amphidromus schomburgki* (Pfeiffer, 1860), Khao Kiew, Thailand, VIS. **J–L.** *Helicostyla ventricosa nobilis* Reeve, 1848, Panay Island, Philippines, VIS (**J**), composite of NUV and transmitted NIR (**K**) and composite of incident NIR and transmitted NIR (**L**). **M–O.** *Papuina buehleri* (Rensch, 1933), Manus I., Admiralty Islands, Papua New Guinea, VIS (**M**), composite of NUV and transmitted NIR (**N**) and composite of incident NIR and transmitted NIR (**O**). **P.** *Otala punctata* (Müller, 1774), La Paloma de Rocha, Uruguay, composite of NUV and transmitted NIR.

not display absorption in incident NIR (Fig. 4C, G). A characteristic shared by the green-shelled tree snails investigated in this paper was their high absorption in the NUV (Fig. 4A, E).

NUV and NIR absorption by periostracum

Among land snails that ordinarily live among grass or bushes, as well as on trees, it is common to observe a uniformly tan or light brown periostracum in VIS. The underlying shell may or may not carry a visible colour pattern, and in some cases this underlying colour pattern may be difficult to observe through an undamaged periostracum. Snails with this type of periostracum generally displayed a very dark periostracal surface in the NUV (Figs 4I–L, 5A–G), which completely obscured any underlying shell colour pattern. The camaenid *Phoenicobius aratus* was a further example. Incidentally, the cyclophorid illustrated in Figure 5A–C showed a distinct colour pattern in VIS (hidden in the NUV by a periostracum opaque to these wavelengths) but, unlike the species discussed in the preceding section, no differential NIR transmission matched the inverse of the colour pattern. All helicid and bradybaenid species

imaged alive and listed in the materials section displayed a strongly NUV-dark periostracum, except when the latter was worn out in old, fully grown individuals.

The camaenid tree snail *Amphidromus schomburgki* (Figs 1I, 5H–K) displayed an unusual periostracal colour pattern, consisting of green collabral bands. Those bands were displayed in enhanced contrast in the NUV, and were faintly visible in both incident and transmitted NIR. The periostracum of the illustrated specimen peeled off in patches, as shown by the fact that some of the colour bands do not extend uninterrupted from the suture to the anterior margin. The shell underneath the periostracum, as visible in these areas of missing periostracum, was uniformly off-white. The periostracal colour bands were translucent green both in incident and in transmitted VIS, and appeared darker than the shell surface in both incident and transmitted NIR.

Reflective white periostracal patterns

Several species of Bradybaenidae displayed spatially nonuniform VIS patterns, consisting of white markings on a uniformly coloured
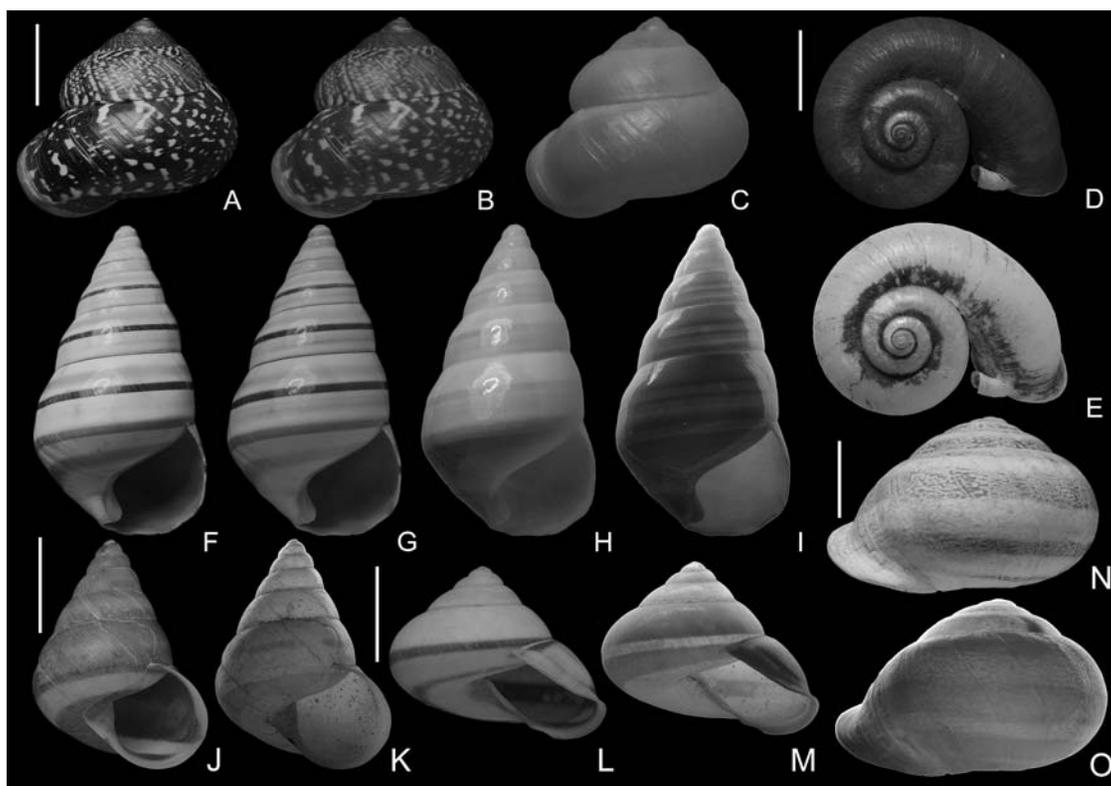
Figure 2. A–C. *Cyclohelix kibleri* Fulton, 1907, Nias Island, Sumatra, Indonesia, NUV (**A**), VIS (**B**) and incident NIR (**C**). **D–E.** *Rhiostoma hainesi* (Pfeiffer 1862), Chantaburi Province, Thailand, VIS (**D**) and incident NIR (**E**). **F–I.** *Liguus virgineus* (Linnaeus, 1758), Dominican Republic, NUV (**F**), VIS (**G**), incident NIR (**H**) and transmitted NIR (*I*). **J–K.** *Papuina chancei* (Cox, 1870), Bismarck I., Papua New Guinea, VIS (**J**) and transmitted NIR (**K**). **L–M.** *Papuina gamelia* (Angas, 1867), VIS (**L**) and transmitted NIR (**M**). N, O, *Otala lactea* (Müller, 1774), Ferry Point Park, Bermuda, VIS (**N**) and transmitted NIR (**O**). Scale bars = 10 mm.
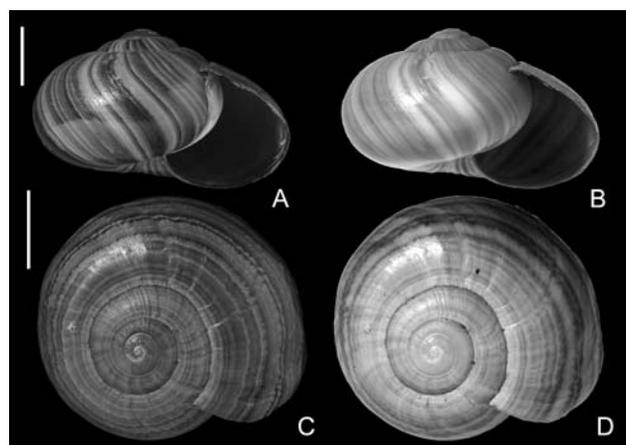

Figure 3. A, B. *Paryphanta lignaria* (Hutton, 1880), South Island, New Zealand, VIS (**A**) and incident NIR (**B**). **C, D.** *Paryphanta* (or *Powelliphanta*) *hochstetteri anatokiensis* (Powell, 1938), central Southern Alps, New Zealand, VIS (**C**) and incident NIR (**D**). Specimens from the Chiba Prefectural Museum of Natural History, Chiba, Japan. Scale bars = 10 mm.

(tan or brown) background (Figs 1J–L, 6, 7). In images, the white areas were considerably lighter than the surrounding surfaces. Common to these species was the fact that the white areas were physically overlaid, as part of the periostracum, onto a darker underlying shell. In some cases, the white portions of periostracum were in slight relief and could be felt by touch.

The NUV properties of those periostracal white patterns varied within this family. In most studied species, the white regions were very light in the NUV (Figs 6A, E, 7A). However, *Calocochlia cumingii* and *Chrysallis* cf. *caniceps* differed in displaying a strong NUV absorption by the outermost layer of periostracum that almost completely hid the light areas (Fig. 7E). In a few Bradybaenidae, including *H. partuloides* (Fig. 7A–D), periostracal, growth-unconformable (*sensu* Seilacher, 1972) white markings were overlaid onto one or more dark spiral lines on the shell surface. This type of dark shell colour pattern was also common among bradybaenids that lacked a white periostracal pattern.

The white periostracal markings of the Bradybaenidae were not unique among land snails. Comparable features were present also in a few representatives of the Helicidae, Orthalicidae, Camaenidae and Enidae (see below). With the important exception of the Bradybaenidae, and possibly of the Camaenidae, only a small subset of species within each of these families displayed this character. Scraping the periostracum removed these white features. These molluscs displayed a determinate growth of the shell, with a reflected outer lip that marked the end of shell growth. Often, the base of the last whorl of adults, in proximity of the aperture, displayed a patch where the periostracum was worn out, likely by friction and continuous contact against the extended soft parts. Small accidental scratches that removed the periostracum from other shell areas were also common (e.g. Figs 1J, 6E, F, I–L).

Bradybaenids displayed a growth-conformable pattern of white spiral bands (Fig. 6A–D), or alternatively a growth-un-conformable pattern of oblique or almost collabral white bands (Figs 1J–L, 6E–L, 7). These features displayed a broad inter- and
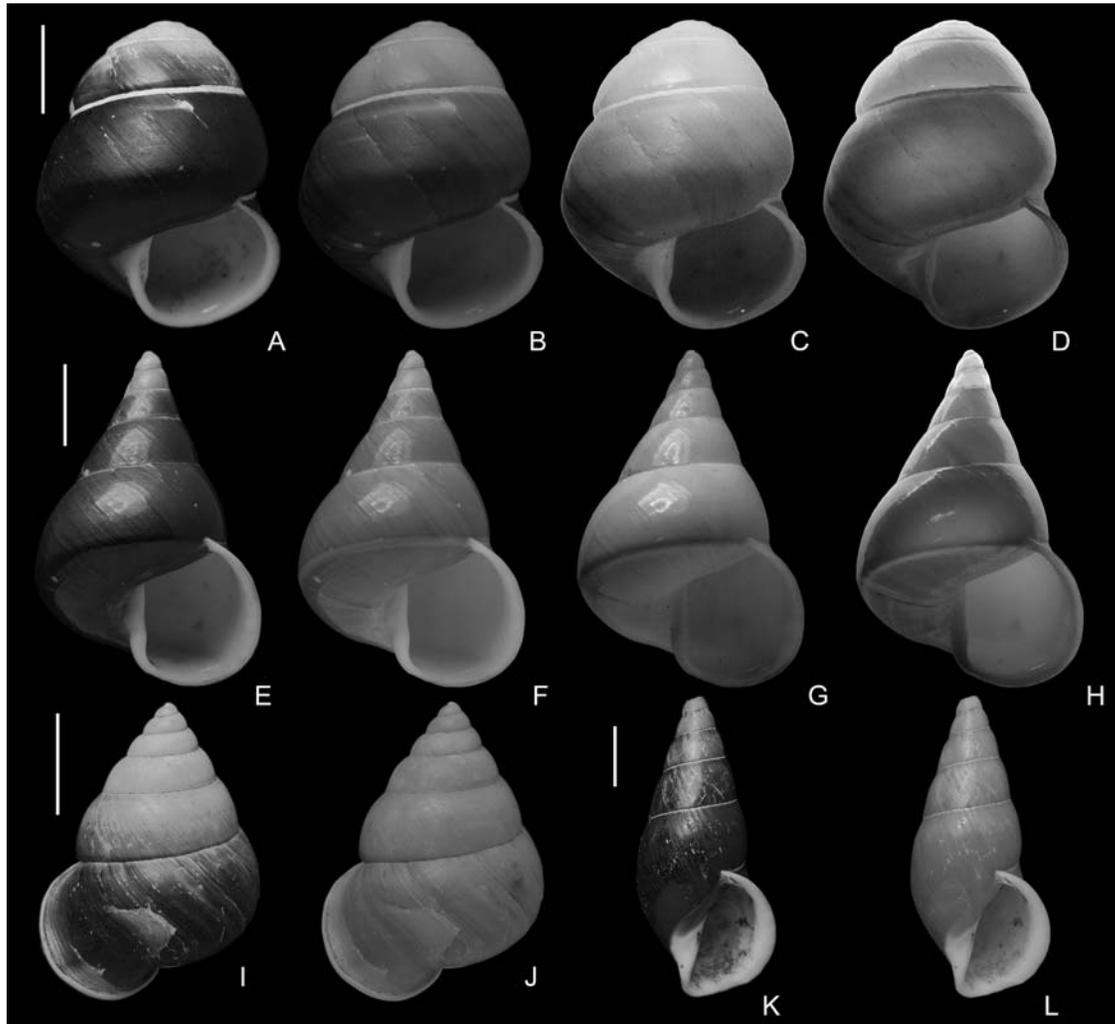
Figure 4. A–D. *Helicostyla florida* (Sowerby, 1841), Mindoro I., Philippines, NUV (**A**), VIS (**B**), incident NIR (**C**) and transmitted NIR (**D**). **E–H.** *Papustyla pulcherrima* Rensch, 1931, Manus I., Papua New Guinea, NUV (**E**), VIS (**F**), incident NIR (**G**) and transmitted NIR (**H**). **I–J.** *Papuina acmella* (Pfeiffer, 1860), Solomon Is, NUV (**I**) and VIS (**J**). **K–L.** *Helicostyla* cf. *virgata* (Jay, 1839) form *porracea* (Jay, 1839), Mindoro Island, Philippines, NUV (**K**) and VIS (**L**). Scale bars = 10 mm.

intraspecific variability. Conspecific individuals in some species ranged from being largely devoid of white markings to being almost completely covered in them. In our material, however, a spatially nonhomogeneous pattern was always present, and we never observed a complete, featureless white coating of the whole periostracal surface.

Reflective white shell patterns

The helicid *Otala lactea* (Fig. 2N, O) probably owes its species name to the fact that the exterior of its shell is coated with an uneven external layer of whitish appearance, rather similar to a spray of milk droplets. Closely comparable features are evident in other species of *Otala*, including *O. punctata* (Figs 1P, 10G–H) and *O. fauxnigra*. In these species, the milky outer layer reflected incident radiation in NUV, VIS and NIR images alike, and was opaque to all transmitted radiation. All species with these features studied by the authors originated from arid or semi-arid environments.

At least one species of the orthalicid genus *Bostryx* (Fig. 9A–D) displayed an external, nonuniform white coating closely similar in reflective properties to the one of *Otala* species. Also in that case, the white markings were opaque to transmitted radiation,

and were apparently located within the outer shell layer. Several species of the camaenid genus *Papuina* displayed a white spatial pattern reflective at all used wavelengths and opaque to transmitted NIR (Fig. 8A–L). In Figure 8C, note that the white stripes were rendered as light-coloured on the adapical portion of the last whorl, but dark on its abapical region. This was an artefact caused by the high convexity of the shell and its high translucence to NIR radiation. These properties caused the abapical region to be predominantly illuminated by NIR transmitted through the shell, while the adapical region received incident NIR. In this species, it may also be noted that the stripes in the abapical region of the last whorl were only barely detectable in NUV and VIS images, but evident in NIR (Fig. 8A–D). These reflecting features in camaenid species were located in the outer shell layer and were often masked in the NUV (especially on the last whorl) by a NUV-opaque periostracum (e.g. Fig. 8E, I).

The enid *Pupinidius melinostoma* (Fig. 9E–H) displayed a striking growth-unconformable pattern of white bars on a brown background. Also in this case the pattern was caused by white markings located in the outermost shell layer, which strongly reflected radiation at all used wavelength bands and consequently were imaged as dark in transmitted NIR.
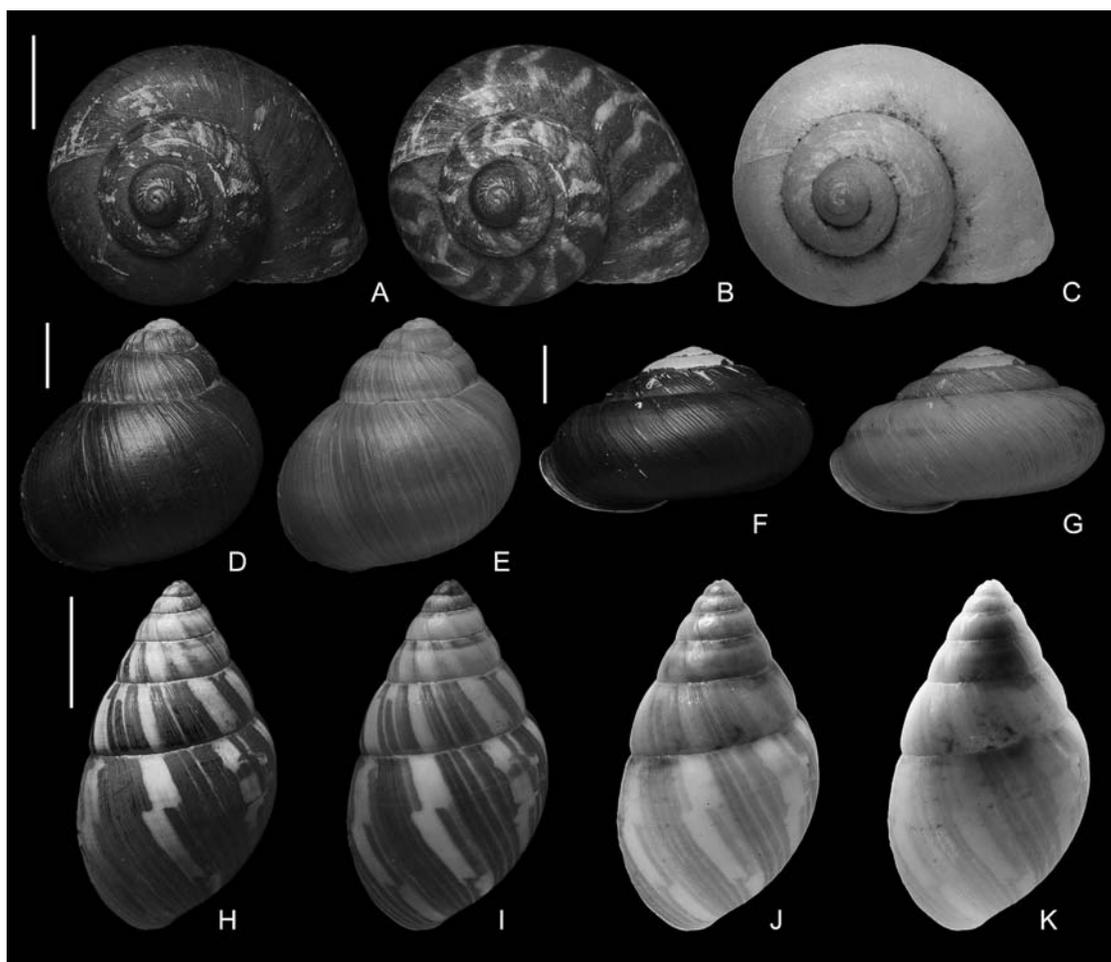
Figure 5. A–C. *Cyclophorus daraganicus* (Hidalgo, 1888), Mindanao, Philippines, NUV (**A**), VIS (**B**) and incident NIR (**C**). **D, E.** *Helix pomatia* Linnaeus, 1758, Uppsala, Sweden, NUV (**D**) and VIS (**E**). **F, G.** *Euhadra* sp., Kyoto, Japan, NUV (**F**) and VIS (**G**). **H–K**. *Amphidromus schomburgki* (Pfeiffer, 1860), Khao Kiew, Thailand, NUV (**H**), visible (**I**), incident NIR (**J**) and transmitted NIR (**K**). Scale bars = 10 mm.

Uniformly white shells

In several observed species, the shell surface was intensely white. In these species, the shell could be uniformly white or displayed faint shell colour markings that covered a minor portion of the shell surface. Several species of Sphincterochilidae fell in this category (e.g. Fig. 10A, B).

DISCUSSION

Solar spectrum

The spectral distribution of solar radiation at ground level is highly variable. Local factors, including latitude, height above sea level, hour and weather conditions contribute to this variability. Nonetheless, it can be stated that, in general, the highest peak in radiation energy reaching the ground level lies between *c*. 500 and 600 nm, i.e. roughly at the centre of the VIS range (Yamamoto, 1962; Gautier, O'Hirok & Ricchiazzi, 1999). Approximately 50% of the total solar energy lies in the VIS.

The energy distribution through the NIR decreases slowly with increasing wavelength, and is still relatively high at 1,000 nm. However, the NIR solar spectrum is not continuous but displays gaps caused by atmospheric absorption. Within the wavelength range of interest for this study, the main gaps are located at *c*. 720, 810 and 940 nm (Yamamoto, 1962;

Gautier *et al.*, 1999). NIR contributes *c*. 45% of the total solar radiation energy at ground level.

Radiation levels rapidly decrease at wavelengths lower than 450 nm, and only *c*. 5% of solar radiation energy is contributed by NUV. The biological effects of NUV, however, are considerable because individual NUV photons are highly energetic. The thermal IR component of solar radiation at ground level does not contribute a substantial portion of incident solar energy (Gautier *et al.*, 1999).

Although the thermal effects of absorbed solar VIS radiation on organisms have been studied (see the Discussion section on white shells in land snails), less attention has been paid to the corresponding effects of solar NIR. There is increasing evidence that the latter are important, as shown, for instance, by recent commercial research on NIR-reflective pigments (see review by Bendiganavale & Malshe, 2008). It was found, for example, that it is feasible to lower the temperature of buildings and other artificial structures exposed to sunlight by coating them with black or dark types of paint that absorb most VIS, as long as these paints are engineered to reflect NIR. Thermal IR emittance (not taken into account in the present study) can also be engineered to enhance the cooling effect.

Vision range of potential predators

Since predation is an important factor in the ecology of many terrestrial snails (Barker, 2004), it is legitimate to ask whether
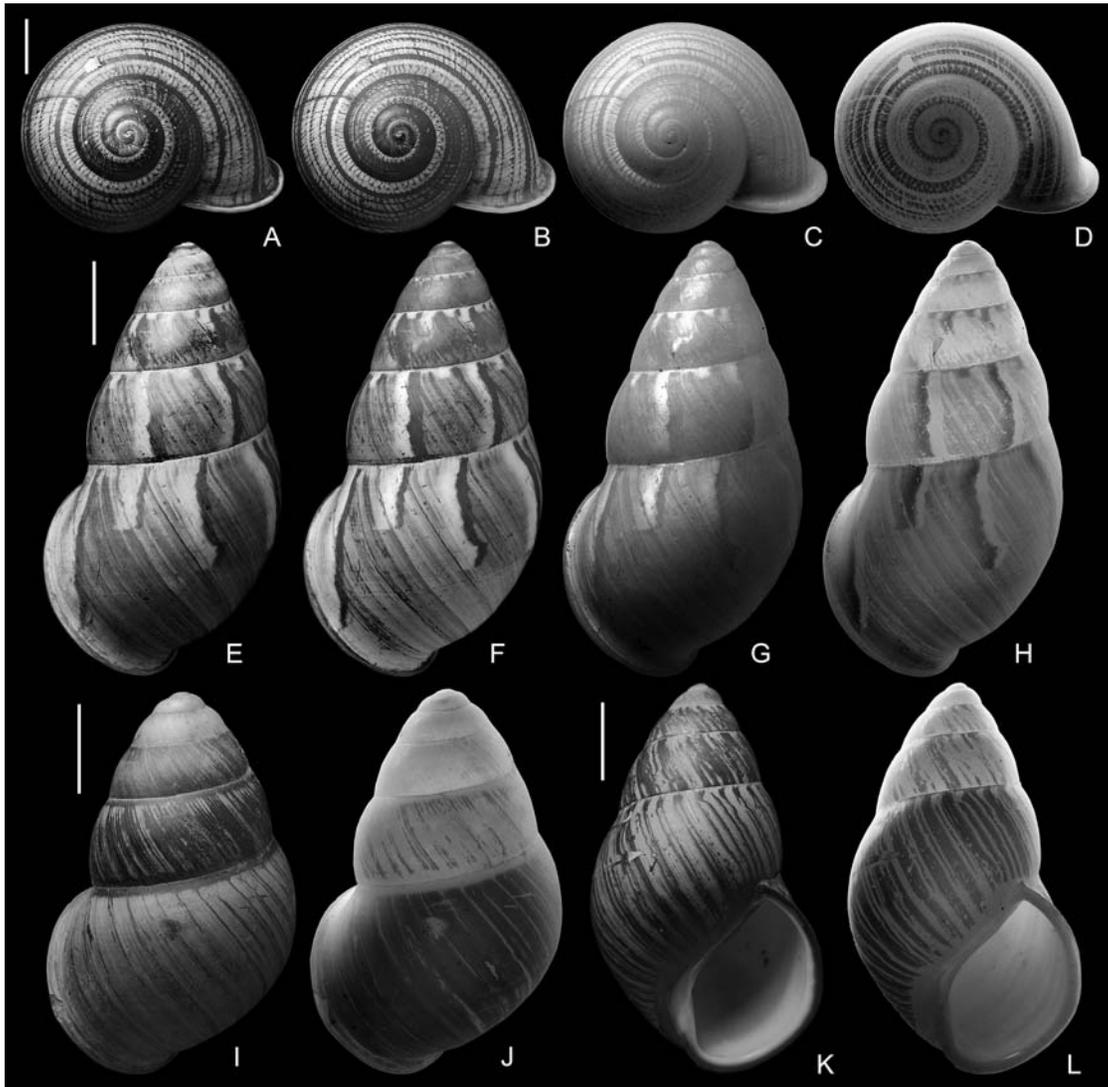
Figure 6. A–D. *Calocochlia festiva* (Donovan, 1825), Cagayan Province, Luzon, Philippines, NUV (**A**), VIS (**B**), incident NIR (**C**) and transmitted NIR (**D**). **E–H.** *Helicostyla ventricosa nobilis* Reeve, 1848, Panay I., Philippines, NUV (**E**), VIS (**F**), incident NIR (**G**) and transmitted NIR (**H**). **I–J.** *H. satyrus* (Broderip, 1841), Balabac I., Philippines, VIS (**I**) and transmitted NIR (**J**). **K–L.** *H. mantangulensis* (Bartsch, 1919) (or possibly a morph of *H. satyrus*), Mantangules I., Palawan, Philippines, VIS (**K**) and transmitted NIR (**L**). Scale bars = 10 mm.
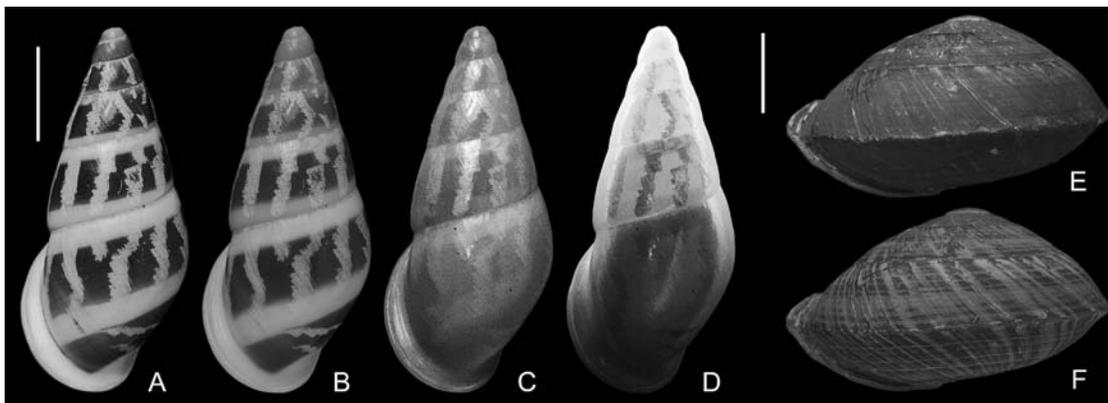

Figure 7. A–D. *Helicostyla partuloides* (Broderip, 1892), Philippines, NUV (**A**), VIS (**B**), incident NIR (**C**) and transmitted NIR (**D**). **E, F.** *Calocochlia cumingii* (Pfeiffer, 1842), Cebu I., Philippines, NUV (**E**) and VIS (**F**). Scale bars = 10 mm.
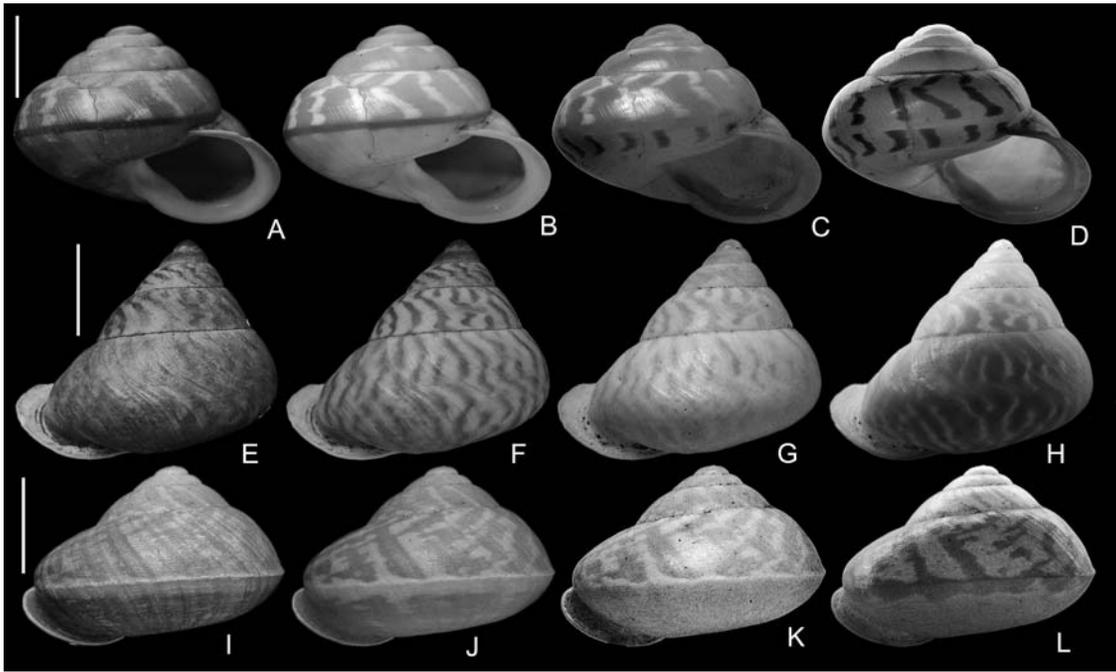
Figure 8. A–D. *Papuina buehleri* (Rensch, 1933), Manus I., Admiralty Is, Papua New Guinea, NUV (**A**), VIS (**B**), incident NIR (**C**) and transmitted NIR (**D**). **E–H.** *P. admiralitatis* (Rensch, 1931), Manus I., Admiralty Is, Papua New Guinea, NUV (**E**), VIS (**F**), incident NIR (**G**) and transmitted NIR (**H**). **I–L.** *Papuina* sp., Manus I., Admiralty Is, Papua New Guinea, NUV (**I**), VIS (**J**), incident NIR (**K**) and transmitted NIR (**L**). Scale bars = 10 mm.
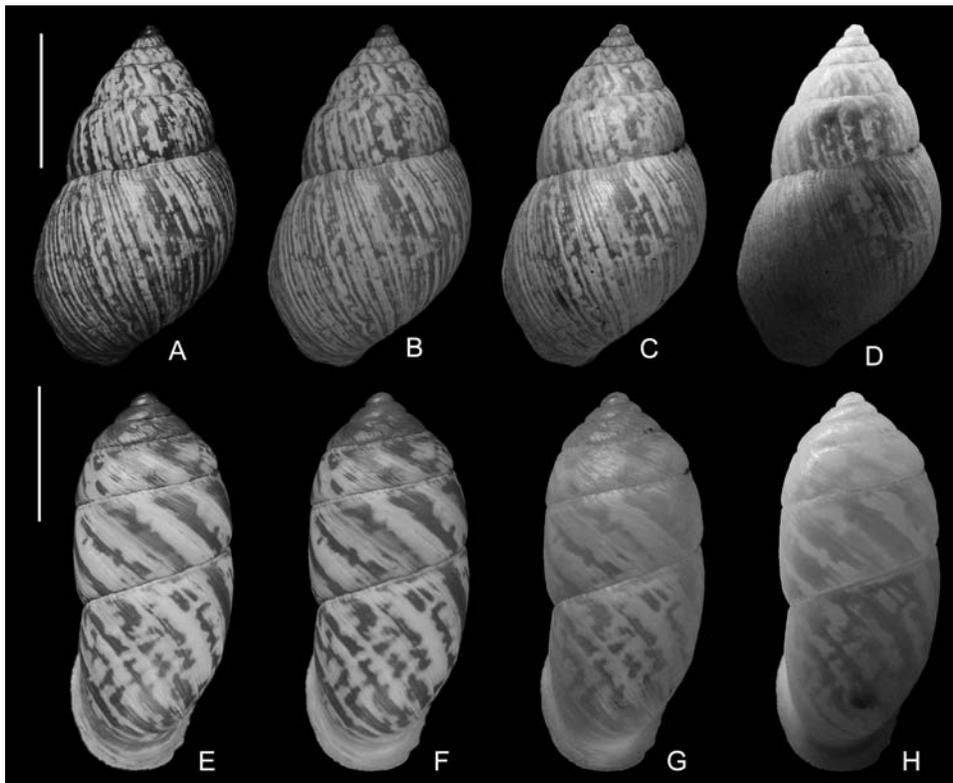

Figure 9. A–D. *Bostryx* sp., Las Lomitas, Parque Pan de Azúcar, Charañal, Región III, Chile, NUV (**A**), VIS (**B**), incident NIR (**C**) and transmitted NIR (**D**). **E–H.** *Pupinidius melinostoma* (Möllendorff), Gansu Province, China, NUV (**E**), VIS (**F**), incident NIR (**G**) and transmitted NIR (**H**). Scale bars = 10 mm.
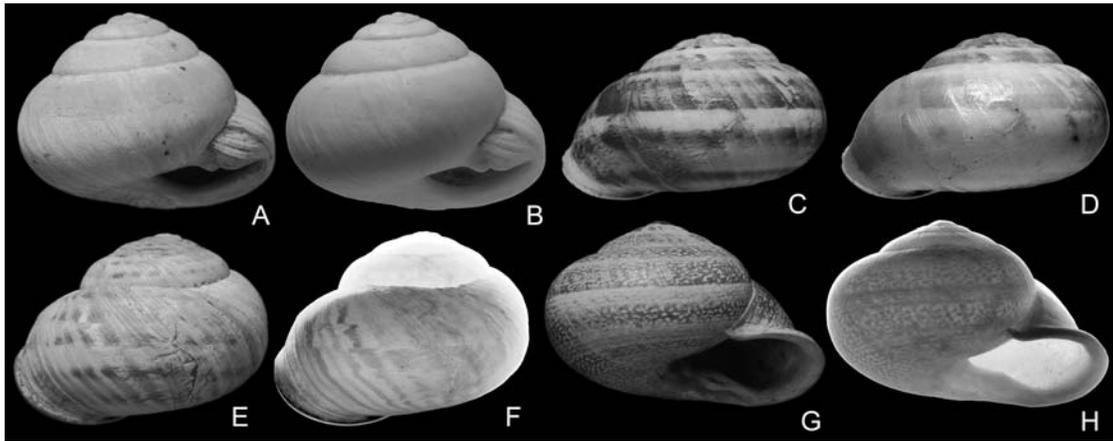
Figure 10. A–B. *Sphincterochila zonata* (Bourguignat, 1853), south of Dimona, Negev, Israel, NUV (**A**), and incident NIR (**B**). **C, D.** *Eobania vermiculata* (Müller, 1774), Split, Croatia, NUV (**C**), and incident NIR (**D**). **E–F.** *Levantina werneri* (Kobelt, 1889), Barequet, Israel, NUV (**E**) and transmitted NIR (**F**). **G–H.** *Otala punctata* (Müller, 1774), La Paloma de Rocha, Uruguay, NUV (**G**), transmitted NIR (**H**) and detail of base of last whorl in VIS (I). Scale bars = 10.

some of the observed optical properties of snail shells provide a form of camouflage or avoidance signal against potential predators. At least some predators are known to display preferences for specific shell colour morphs of terrestrial snails (Slotow, Goodfriend & Ward, 1993; Rosin *et al.*, 2011). This does suggest that visual cues are used by these predators to select their prey.

Vision in the NUV is documented in several terrestrial organisms, especially birds (e.g. Kreithen & Eisner, 1978; Emmerton & Delhis, 1980; Cuthill *et al.*, 1997; Bennett *et al.*, 1997) and pollinating insects such as bees and butterflies (e.g. Horridge, 2009). Many insect-pollinated flowers display a high NUV reflectivity and/or high-contrast NUV patterns, often not apparent in VIS, functional in attracting a broad range of pollinating insects and birds (e.g. Primack, 1982; Dieringer, 1982; Biedinger & Barthlott, 1993; Medel, Botto-Mahan & Kalin-Arroyo, 2003; Leonard & Papaj, 2011). Although these pollinating species obviously are not snail predators, the widespread presence of NUV vision among insects and birds does suggest that it may be present also among snail predators.

Diurnal mammals are typically insensitive to NUV and the crystalline lens and vitreous humour of their eyes largely absorb these wavelengths (Müller *et al.*, 2009). The main adaptive value of this trait is believed to be protection against damage by high-intensity radiation at these wavelengths (Müller *et al.*, 2009). NUV vision has been proposed or documented for certain bats, rodents and a few other mammals that are active at night or around down and dusk, i.e. when the overall light intensity is lower than during the day, but NUV levels are proportionally higher (Jacobs, Neitz & Deegan, 1991; Calderone & Jacobs, 1999; Yokoyama & Shi, 2000; Arrese *et al.* 2002; Chávez *et al.*, 2003; Winter, López & Von Helverson, 2003; York, López & Von Helverson, 2003; Peichl *et al.*, 2005; Williams, Calderone & Jacobs, 2005; Fure, 2006; Müller *et al.*, 2009).

Several crustaceans are known to be capable of NUV vision, including land crabs and semi-terrestrial amphipods (e.g. Lall & Cronin, 1987; Ugolini *et al.*, 2010). Some of these crustaceans may potentially feed on land snails. NUV vision is also documented in spiders (e.g. Lim & Li, 2006). Land snail predation by spiders was studied by Breure (2011).

There appear to be no documented instances of vision in the NIR range by terrestrial organisms. Early reports of NIR, and even deep-IR, vision in nocturnal predatory birds (e.g. Vanderplank, 1934) have been dismissed by subsequent findings that vision in these birds does not extend into the infrared (Hecht & Pirenne, 1940; Hocking & Mitchell, 2008). The apparent sensitivity of certain owl species to NIR under laboratory conditions (Vanderplank, 1934) most likely was caused by low-level VIS leaking through the NIR-pass filters used in the experiments (Hecht & Pirenne, 1940), while the capability of these birds to catch living prey in complete darkness relies on sound detection, rather than thermal-IR detection (Hecht & Pirenne, 1940; Payne, 1971; Martin, 1986).

The general lack of biological NIR vision has been justified by the finding that vision pigments produce increased signal noise as wavelength increases (Luo *et al.*, 2011). At NIR wavelengths, noise overwhelms the useful signal (Luo *et al.*, 2011). Nonetheless, a few modern reports do indicate at least a marginal detection of NIR at wavelengths up to 870 nm, e.g. in ferrets (Newbold & King, 2009). A simple detection of radiation, however, does not equate to a useful image-forming vision or image recognition at these wavelengths. It is also possible that the NIR radiation detected by these organisms under laboratory conditions would be entirely masked out by the sensory effects of other wavelengths under natural conditions. The multiple gaps in solar radiation in the NIR, mentioned in the section on solar radiation, are a further factor that may limit the potential usefulness of biological NIR detection. Thus, it appears that NIR vision, even in the lack of signal noise, would be of little use in allowing a predator to detect land snails among vegetation.

This discussion does not include the biological detection of thermal IR, which exploits longer wavelengths and does not involve eyes and their radiation-sensitive pigments. Thermal IR is also beyond the recording range of the equipment used in this paper.

NUV reflectivity of natural substrates

Data on the reflectivity of NUV by natural substrates are available (e.g. Verhoeven & Schmitt, 2010). Tree foliage, and green vegetation in general, is normally very dark in reflected NUV, and completely opaque to transmitted NUV (Grant *et al.*, 2003; Yoshimura *et al.*, 2010; E. Savazzi, pers. obs.). Rock and bark are generally lighter than green vegetation in reflected NUV (E. Savazzi, pers. obs.).

11

NIR reflectivity of natural substrates

The NIR reflectivity of land vegetation, like its NUV reflectivity, has been studied for military and remote-sensing purposes (e.g. Campbell, 2002). Most deciduous vegetation that appears green in the visual range strongly reflects in the NIR. This is caused by reflection by the spongy mesophyll structure and by the NIR translucence of surrounding leaf tissues (Campbell, 2002).

The amount of NIR reflection by green vegetation is much higher than in VIS, and differs among vegetation types. For instance, a NIR reflection (at 800 nm) of *c*. 85% was reported for grass, 50% for deciduous forest trees and 25% for coniferales (Campbell, 2002). Reflection of green light (550 nm) of the same vegetation types is *c*. 10%, 15% and 8%, respectively (Campbell, 2002).

Certain sediment types, like quartz sand, are highly NIR-reflective (E. Savazzi, pers. obs.). Soil is often imaged as very dark and opaque in the NIR (e.g. the soil particles in Fig. 2E).

Dark shell colour patterns in VIS and NUV

Shell colour patterns in VIS are extremely common among land snails. These patterns usually consist of dark bands, spots or patches on an even background, often white or whitish. The dark elements of shell colour patterns in VIS examined here were almost invariably rendered in NUV as darker than in VIS. Conversely, white, apparently nonpigmented shell surfaces were rendered in NUV as more reflective and less translucent than in VIS. These properties combined to enhance the contrast between dark and light areas of these patterns in NUV images (unless the shell was overlaid by an NUV-opaque periostracum).

Dark shell colour in NIR

In most observed species, dark elements of VIS shell colour were imaged as translucent and undetectable, or almost undetectable, in NIR. The shell in NIR images appeared evenly light coloured and more translucent than in VIS. The Rhytididae (Fig. 3B, D) displayed examples of a dark VIS shell colour pattern that were also imaged as dark in NIR (albeit to a lesser extent than in VIS). Only green or black colour lines or bands, however, displayed this behaviour, while red and brown elements were undetectable in NIR images. This suggests the possible simultaneous presence of multiple types of pigments or structural colour. According to the summary by Murray (1998), these Rhytididae are carnivorous, normally found under detritus and stones, and often nocturnal. They are eaten by predatory mammals and birds (Murray, 1998).

The NIR properties of the shell colour pattern observed in species of the Rhytididae remain unexplained from an adaptive point of view. Since these species are not normally exposed to sunlight for extended periods, a high NIR reflectivity is likely not adaptive to lower the body temperature, and the observed NIR absorption by shell pigments may be a nonadaptive consequence of the evolutionary 'choice' of colours that are adaptive as camouflage in VIS.

The caryodid *Pedinogyra hayii* from Australia was comparable in shell geometry, size and VIS colour to the above Rhytididae, as well as in possibly nocturnal habits (at least judging from other caryodid species, e.g. Murphy, 2002). However, its shell colour is undetectable in NIR.

Uniformly NUV-dark shell colour

A few species of bradybaenid and camaenid tree snails displayed a uniform green colour of the shell. This VIS colour suggests a background-matching VIS camouflage against green vegetation. The same shells were very dark in NUV (Fig. 4A, E), but highly reflective in NIR (Fig. 4C, G). This matched well the NUV properties of green vegetation and further suggests that background-matching camouflage in these species extends into the NUV.

Uniformly NUV-dark periostracum

Land snails with uniformly yellow or tan periostraca in VIS displayed a strongly NUV-absorbing periostracum, which was very dark in this wavelength range (Figs 4I–L, 5A–G). This type of periostracum also hid any underlying shell colour pattern in NUV, even when evident in VIS. The NUV-dark periostracum may be a background-matching camouflage against vegetation. When associated with prevalently brown shell colour (evident in VIS, but not NUV), this combination suggests that the VIS pattern or colour had a function as either disruptive camouflage, or background-matching camouflage against wood and dead leaves.

An NUV-absorbing periostracum, at least in the observed species, is not likely to be functional in protecting the soft tissues contained in the shell from exposure to NUV radiation, because the shell itself, even when thin and relatively translucent in VIS, completely blocks transmitted NUV. In the material illustrated in this paper, this property is shown by the consistently darker appearance of the interior of the shell aperture in NUV, compared with VIS and (especially) NIR. However, it cannot be excluded that an NUV-absorbing periostracum may have this adaptive value in extremely thin and translucent shells. Exceptions to uniformly NUV-dark periostraca do occur, and are discussed in the following sections.

NIR-dark periostracal colour patterns

The green periostracal colour bands of *Amphidromus schomburgki* (Figs 1I, 5H–K) are darker than adjacent regions in both incident and transmitted NIR images. This NIR behaviour is comparable with the shell colour pattern of the Rhytididae.

White periostracal patterns

A variety of periostracal colour patterns was present among numerous Bradybaenidae. In those species, the patterns consisted of white periostracal features superposed onto a darker shell. The NUV behaviour of those patterns varied, with most species displaying NUV reflectivity matching the VIS pattern. However, in a few species the white pattern seemed to be covered by a thin layer of periostracum, translucent in VIS, but sufficiently opaque in NUV to completely hide the underlying pattern. The white periostracal areas were also reflective in NIR, and consequently opaque to transmitted NIR, yielding a negative rendering of the pattern in this illumination type.

In a few species, the white areas had a spatially nonuniform reflectivity, with some portions of the pattern slightly translucent and showing the underlying tan or brown shell and periostracum, and other portions so reflective that they completely hide the underlying darker colour and in some cases even display a detectable amount of directional, specular reflection of the light source in NUV, VIS and, particularly, NIR images (see especially Fig. 6G).

Given that these patterns were spatially nonuniform and high in visual contrast, a function as disruptive camouflage seems likely, at least in NUV and VIS. The lack of documented NIR vision by potential predators seems to exclude this function in NIR. On the other hand, the white elements of this colour pattern often covered most of the total shell area, and a

hypothesis of concomitant functions as camouflage and thermal control can be proposed. This agrees with the fact that most species displaying this type of pattern are either tropical or found in seasonally arid and hot environments, where a reduction in body temperature by enhanced shell reflectance may be advantageous (see also the following section).

White shell patterns

In *Liguus virgineus* (Fig. 2F–I), the spiral colour bands were flanked by slightly thicker, noncoloured shell areas. Those areas were more reflective in incident VIS and NIR than the rest of the shell (and more opaque to transmitted VIS and NIR), and enhanced the contrast between colour bands and noncoloured adjacent areas. The complete translucence of the dark colour bands of *L virgineus* in NIR made the selectively different properties of adjacent shell areas obvious in this wavelength band.

In several species of Camaenidae (Fig. 2J–M), Orthalicidae and Helicidae (Fig. 2N, O), transmitted NIR images were a 'negative' rendering of incident VIS images. Further examples are shown in Figure 8D, H and L. In VIS, the white markings were superimposed onto a dark background colour. This background is translucent in transmitted NIR, and therefore rendered as light in this illumination type. The white markings, on the other hand, displayed an enhanced reflectivity in both VIS and NIR, as well as a low NIR translucence that makes it appear dark in transmitted NIR. The two phenomena combined to enhance the contrast of the colour pattern in incident VIS and NUV, thus suggesting an adaptive value in the context of camouflage.

The visual results produced by white periostracal patterns (discussed in previous section) and white shell patterns were quite similar, and in fact may be difficult or impossible to distinguish without a close examination of the distribution of colour through the periostracum and/or shell. These structurally distinct characters that produce similar contrast patterns may be regarded as an example of convergence.

Function of white markings of periostracum and shell

Given the apparent lack of NIR vision among snail predators (see section on predator vision), the NIR reflectivity of periostracal and shell white markings is unlikely to have a camouflage function in this wavelength band. It remains to explore whether another adaptive significance than camouflage is feasible for the observed high NIR reflectivity. An alternative possibility is that this property may simply not be adaptive in the NIR, and may only be an 'accidental' consequence of its adaptive properties at other wavelengths.

Precise data were not available on the life habits of the species of snails that possessed a reflecting white pattern. Representatives of these families are known to be mostly tropical tree snails (e.g. Cooke, 1892) and the species with reflecting white patterns conform to the general shell sizes and geometries of other representatives of these families from the same geographic areas. We were unaware of any data that would suggest atypical life habits for the species that possess white reflecting patterns.

Tree snails of tropical regions, and particularly species that live near the top of the leaf canopy and/or on trees with thin foliage, can be exposed to high levels of sunlight. Sunlight carries most of its energy in the VIS and NIR (see section on solar spectrum), and the observed white surfaces are effective reflectors in the same spectral interval, especially when they cover most of the shell surface. Thus, in these species and/or morphs the white colour may conceivably be adaptive in reducing the amount of absorbed solar radiation (in addition to the possible camouflage function in VIS), thereby lowering the body temperature in a way comparable with that observed in white-shelled desert snails. This possible function is further discussed in the following section.

The presence of a high-contrast pattern is irrelevant or deleterious to the function of a radiation reflector, since any discontinuities in the reflective coating expose shell areas of lower reflectivity and reduce the total amount of reflected radiation. Thus, the maximum efficiency as a reflector would be attained by a uniform white coating of the shell, as observed in white desert snails (see following section). The common presence of a pattern in the Bradybaenidae does suggest a simultaneous function as camouflage in the NUV and VIS. Even in the presence of a pattern, most of the shell is often white (e.g. Fig. 5A–L) and this is compatible with both functions. However, a simultaneous function of the pattern as camouflage prevents its maximal optimization as a reflector.

Uniformly white shells

Land snails of deserts and arid climates are often subjected to intense sunlight and high temperatures. White, or predominantly white, shells in land snails are often associated with life under intense sunlight, especially during aestivation, and are adaptive in reflecting a major portion of incident sunlight (Schmidt-Nielsen, Taylor & Sholnik, 1971). A maximum temperature of 56.2°C has been recorded within the last whorl of aestivating *Sphincterochila boissieri*, which possesses a chalk-white shell (Schmidt-Nielsen *et al.*, 1971). Since this temperature was lower than the temperature of the surrounding substrate, it was inferred that the high reflectivity of the white shell (over 90% of incident sunlight in VIS, and an estimated 95% in the NIR) is adaptive in preventing overheating, together with the insulating effect of air trapped within the empty last whorl (Schmidt-Nielsen *et al.*, 1971). Other species of *Sphincterochila* live in deserts and seasonally arid environments and have comparable white shells (e.g. Abbes, Nouira & Neubert, 2011).

A white (albeit, to a lesser degree than in the above species) shell in morphs of *Cepaea nemoralis* (Helicidae) yields a lower body temperature than darker shells when the organism is exposed to direct sunlight (Heath, 1975), and this improves the survival of this species (Richardson, 1974). This species is found in a variety of environments, including semi-arid ones (Richardson, 1974; Heath, 1975). Moreno-Rueda (2008) experimentally found that the naturally white shell of the arid-dwelling species *Sphincterochila (Albea) candidissima* reduces the weight loss of individuals during aestivation, with respect to artificially blackened shells. This species remains exposed to sunlight during the dry season (Moreno-Rueda, 2007).

Theba pisana (Helicidae), *Xeropicta derbentina* (Hygromiidae) and *Cernuella* (or *Helicella*) *virgata* (Hygromiidae), originally from hot and seasonally arid circum-Mediterranean environments, display a preference for aestivating on leafless bushes or tree branches exposed to high levels of sunlight (e.g. Pomeroy, 1968; Scheil, Kohler & Triebskorn, 2011). These species possess mostly (albeit, not entirely) white shells and display a high tolerance to heat and seasonally dry environments (Pomeroy, 1968; Scheil, Kohler & Triebskorn, 2011). *Cernuella virgata*, for instance, typically aestivates in full sun on vegetation above ground level (Pomeroy, 1968). Light-coloured morphs of the colour-polymorphic desert dweller *Xeropicta vestalis* are more common in localities where leaf shelter is less available, suggesting a similar adaptive value of light-coloured shells (Heller & Volokita, 1981). *Albinaria caerulea* (Clausiliidae) is exposed to high levels of sunlight during aestivation, and likewise possesses a white shell, believed to be functional in the same way (Giokas, Pafilis & Valakos, 2005). White, or mostly

white, shells are also common among species of the Cerionidae, which commonly live in hot arid and semi-arid environments and often aestivate in positions fully exposed to sunlight (our observations). The thermal effects of solar radiation on artificial structures can be altered by using NIR-reflective paint. This supports the feasibility of the idea that NIR reflectivity of land snail shells may be important in thermal regulation.

Factors other than body temperature and sunlight reflection may also be important to the survival of snail species in arid environments. For instance, Slotow et al. (1993) found that white and brown morphs of *Trochoidea seetzeni* do not differ in body temperature, but brown morphs, in spite of being presumably better camouflaged in their natural environment, are statistically preferred by snail-eating rodents. The evolutionary processes that maintain this colour dimorphism are not clear (Slotow et al., 1993). *Trochoidea simulata* also occurs in white and brown morphs, with white morphs having a thicker shell with higher calcium carbonate content (Slotow & Ward, 1997). This case was explained by different ecological preferences of the morphs, with the white ones being more common on soils richer in calcium carbonate (Slotow & Ward, 1997). Difficulties and inconsistencies are found in the adaptive interpretation of colour di- and polymorphism in land snails of other environments. For instance, Jones (1982) reported that light versus dark colour morphs of *Cepaea nemoralis* expose themselves to different amounts of sunlight. However, Chang & Einlen (1993) concluded that, during the hot and dry season, the distribution of both light and dark morphs in this species tends to be controlled by the availability of shelter, while food distribution is the controlling factor for both morphs during the wet season. Rosin et al. (2011) found that rodent and bird predators of *C. nemoralis*, respectively, display different preferences for colour and size of these snails. Rosin et al. (2011) have reviewed the numerous studies on colour polymorphism in this species.

Among other organisms characteristic of arid environments, the adaptive significance of dark versus light colour may likewise be difficult to interpret. The common occurrence of black colour in desert organisms has been noted by several authors (e.g. Cloudsley-Thompson, 1978). Desert birds seem to be predominantly dark (Ward et al., 2002). In a comparison of two sympatric species of *Onymacris* (Tenebrionidae, Coleoptera) from the Namib Desert, one entirely black and the other with white elytra, body colour was found to affect body temperature as a result of direct illumination by a quartz halogen lamp (Turner & Lombard, 1990). However, heat removal by wind, in this case, had a greater effect on body temperature than direct illumination, and was regarded by Turner & Lombard (1990) as the most important single factor affecting body temperature in these insects.

Isolated reports of especially high NIR reflectivity are available, e.g. in a few reptile and amphibian species (Dodd, 1981; Emerson, Cooper & Ehleringer, 1990). Thermoregulation and camouflage from predators were speculatively mentioned as possible adaptive reasons for a high NIR reflectivity in certain chameleon species by Dodd (1981). Thermoregulation, on the other hand, was rejected for similarly reflective tree frogs by Emerson et al. (1990), on the basis of energy-budget analysis. Camouflage was regarded by the latter authors as a more likely adaptive cause of the convergent high NIR reflection observed among tree frog species. This explanation is incompatible with the apparent lack of biological NIR vision discussed above.

Disruptive camouflage

The adaptive value of many examples of spatially uneven camouflage patterns is believed to lie in a disruption of the visual recognition of a potential prey by predators (e.g. Cuthill & Székely, 2011; Stevens & Merilaita, 2011b). Unlike background-matching camouflage, which is based on a good colour match between prey and substrate, disruptive camouflage works by producing a spatially nonuniform signal. This type of camouflage appears to be effective when the frequency of its spatial signal matches the prevalent spatial signal produced by the background, but neither the amplitude of the signal (i.e. the visual contrast of the pattern) nor the colours of the pattern need to precisely match the substrate (Godfrey, Lythgoe & Rumball, 1987). A mismatch in signal frequencies, on the other hand, may make the potential prey more easily detectable (Godfrey et al., 1987).

The colour patterns of many species of land snails in the NUV and VIS would seem to qualify as disruptive camouflage. This includes the very common patterns of spiral lines (e.g. Figs 2F, G, J, L, 3, C, 6A−D), as well as other types of patterns discussed below. The visual appearance of Bradybaenidae with growth-unconformable colour patterns (Fig. 6E−H) strongly suggests a 'military-type' disruptive camouflage consisting of irregular patches. Growth-conformable (i.e. spiral or collabral) patterns (Fig. 6A−D), or growth-unconformable patterns that almost comply with a growth-conformable geometry (e.g. Fig. 6I−L) are more easily detected by humans, because of their higher geometric regularity. However, snail predators very likely have different pattern-recognition capabilities than humans, and we are not suggesting that growth-unconformable patterns are particularly effective against the snails' natural predators and in their natural environments. Any such statement would need to be supported by experimental evidence (e.g. Stevens & Merilaita, 2011a; Troscianko et al., 2011). Thus, we restrict our conclusions to stating that all observed types of colour patterns in the Bradybaenidae may be functional as camouflage. Meinhardt (2009) showed that the diverse types of geometric patterns discussed in this paper could result from slight changes in the same, or very similar, underlying physiological mechanisms. Therefore, it is not surprising to find geometrically different types of pattern in closely related species, or even in conspecific morphs.

Other types of camouflage

In the context of camouflage, it should be noted that shell colour and its pattern can be adaptive in other ways than by disrupting the recognition of the organism's shape (see preceding section) or blending into the surrounding environment (i.e. background-matching camouflage, see Stevens & Merilaita, 2011a). For instance, masking as a visually conspicuous but inedible object or organism (masquerading camouflage, see Skelhorn et al., 2010; Skelhorn & Ruxton, 2010, 2011; Stevens & Merilaita, 2011a) or displaying an aposematic colour pattern (Komarek, 1998; Rowe, 2001) may also be effective strategies against predators. Specifically, it may be noted that empty snail shells and pebbles are often common in dry hot environments and, regardless of their original colour, are often bleached by exposure to sunlight. Thus, a white, apparently sun-bleached shell in living individuals, besides being adaptive in the context of thermal regulation as discussed above, could have an additional value in making these individuals difficult for a predator to distinguish visually from empty shells or white pebbles. We are not aware of literature on this hypothesis having being tested, but it could be worth considering (together with alternative explanations, including that white shells may be thicker and/or harder to break than brown ones) in cases like the one reported by Slotow et al. (1993), where brown morphs of *Trochoidea seetzeni* were found to be preferred to white ones by predatory rodents.

The milky-white, uneven shell coating of species of *Otala* (Figs 1P, 10G, H), the comparable appearance of a *Bostryx* species From the Atacama Desert of Chile (Fig. 9A–D) and the 'washed-out' appearance of *Eobania vermiculata*, *Theba pisana*, *Xeropicta derbentina*, *Cernuella virgata* and other helicids of seasonally arid environments (Fig. 10C, D), besides enhancing the shell reflectivity and thereby reducing the thermal effects of solar radiation, could also represent a form of camouflage that mimics the appearance of sun-bleached and corroded empty shells. The light and low-contrast colour patterns that cover a small percentage of the shell surface in these species necessarily reduce its reflectivity (albeit probably by a small amount). Thus, also in these species a compromise seems to exist with regard to optimization of the shell colour for a dual function of sunlight reflector and disruptive camouflage.

These ideas need to be experimentally verified, since alternative explanation may exist. For instance, in environments where snail shells are continuously exposed to intense sunlight, a white shell or a faint colour pattern may evolve as a way to save the energy that would be required for the production of high-contrast colour patterns resistant to this level of irradiation. Intraspecific polymorphism may also play a role in camouflage, since predators that become attuned to a particular colour morph may conceivably disregard other morphs.

CONCLUSIONS

In the majority of land snail species studied here, shell colour patterns that are detectable in VIS appeared in enhanced contrast in NUV and were totally, or almost totally, undetectable in incident NIR images. Species of Rhytididae were exceptions in that their colour patterns were distinct also in incident NIR images.

The periostracum of many (albeit not all) studied species in the Helicidae, Camaenidae and Bradybaenidae strongly absorbed NUV and appeared very dark in NUV images. This characteristic matches the typical appearance of green vegetation in the NUV and may therefore be a form of background-matching camouflage. Many of the species with NUV-opaque periostraca possessed colour patterns easily detectable through the periostracum in VIS, but as a rule undetectable in NUV.

Land snails of desert and arid climates often have wholly or mostly white shells, highly reflective at all studied wavelengths and apparently effective as reflectors of solar radiation. White shells in these snails may also constitute a form of masquerading camouflage that makes the shells of living individuals visually similar to empty, sun-bleached shells and white pebbles.

In several species of Helicidae, Orthalicidae and Camaenidae, shells with dark spiral bands in VIS also displayed a heightened reflectivity of adjacent, light shell regions. This is particularly noticeable in transmitted NIR images, in which the shell pigments were not detectable and the reflective areas were opaque to NIR, thus yielding an inverted, or 'negative' image of the colour pattern. These features enhanced the contrast of the colour pattern in incident VIS (and, to a lesser extent, in incident NUV) and may be adaptive as camouflage, but seemed to lack obvious functions in the NIR. At least in some species, the regions of enhanced reflectivity corresponded to a slightly increased shell thickness, compared with the adjacent dark areas.

Areas that reflected light to a higher extent than surrounding regions, and appeared white or whitish in VIS, formed a variety of geometric patterns on the periostracum or shell of several species of Bradybaenidae and, less frequently, Camaenidae, Orthalicidae, Helicidae and Enidae. Unlike typical dark shell pigments, this white colour stood out as more reflective than its background in NUV, VIS and reflected NIR images. This white colour pattern may have a dual adaptive function as

disruptive camouflage (in the NUV and VIS) and as a reflector of solar radiation (in VIS and NIR) to lower the internal shell temperature. The first of these functions likely prevents a full optimization of the white pattern as a reflector of solar radiation, which would be maximized by a complete and homogeneous white coating of the shell.

REFERENCES

ABBES, I., NOUIRA, S. & NEUBERT, E. 2011. Sphincterochilidae from Tunisia, with a note on the subgenus *Rima* Pallary, 1910 (Gastropoda, Pulmonata). *Zookeys*, **151**: 1–15.

ANDERSSON, S. & AMUNDSEN, T. 1997. Ultraviolet colour vision and ornamentation in bluethroats. *Proceedings of the Royal Society of London, Series B*, **264**: 1587–1591.

ARRESE, C.A., HART, N.S., THOMAS, N., BEAZLEY, L.D. & SHAND, J. 2002. Trichromacy in Australian marsupials. *Current Biology*, **12**: 657–680.

BARKER, G.M. (ed.) 2004. *Natural enemies of terrestrial molluscs*. CABI, Wallingford, UK.

BENDIGANAVALE, A.K. & MALSHE, V.C. 2008. Infrared reflective inorganic pigments. *Recent Patents on Chemical Engineering*, **1**: 67–79.

BENNETT, D., CUTHILL, I.C. & PARTRIDGE, L.K. 1997. Ultraviolet plumage colors predict mate preferences in starlings. *Proceedings of the National Academy of Science of the USA*, **94**: 8618–8621.

BIEDINGER, N. & BARTHLOTT, W. 1993. Untersuchungen zur Ultraviolettreflexion von Angiospermenblüten. 1 Monocotyledoneae. *Tropical und Subtropical Pflanzenwelt*, **86**: 1–122.

BREURE, A.S.H. 2011. Dangling shells and dangerous spiders: malacophagy and mimicry in terrestrial gastropods. *Folia Conchyliologica*, **7**: 7–13.

CALDERONE, J.B. & JACOBS, G.H. 1999. Cone receptor variations and their functional consequences in two species of hamster. *Vision Neuroscience*, **16**: 53–63.

CAMPBELL, J.B. 2002. *Introduction to remote sensing*. Edn 3. Guilford Press, New York.

CHANG, H.W. & EINLEN, J.M. 1993. Seasonal variation of microhabitat distribution of the polymorphic land snail *Cepaea nemoralis*. *Oecologia*, **93**: 501–507.

CHÁVEZ, A.E., BOZINOVIC, F., PEICHL, L. & PALACIOS, A.G. 2003. Retinal spectral sensitivity, fur coloration, and urine reflectance in the genus *Octodon* (Rodentia): implications for visual ecology. *Investigative Ophthalmology and Visual Science*, **44**: 2290–2296.

CLOUDSLEY-THOMPSON, J.L. 1978. Adaptive function of the colors of desert animals. *Comparative Physiological Ecology*, **1**: 109–120.

COMFORT, A. 1951. The pigmentation of molluscan shells. *Biological Reviews*, **26**: 285–301.

COOKE, A.H. 1892. On the geographical distribution of the land-Mollusca of the Philippine Islands, and their relations to the Mollusca of the neighbouring groups. *Proceedings of the Zoological Society of London*, **60**: 447–508.

CUTHILL, I.C., PARTRIDGE, J.C., BENNETT, A.T.D., CHURCH, S.C., HART, N.S. & HUNT, S. 1997. Ultraviolet vision in birds. In: *Advances in the study of behavior*. Vol. 29. (P.J.B. Slater, J.S. Rosenblatt, C.T. Snowdon & T.J. Rope, eds), pp. 159–214. Academic Press, San Diego, CA.

CUTHILL, I.C. & SZÉKELY, A. 2011. The concealment of body parts through coincident disruptive coloration. In: *Animal camouflage: mechanisms and function* (M. Stevens & S. Merilaita, eds), pp. 34–52. Cambridge University Press, Cambridge, UK.

DIERINGER, G. 1982. The pollination ecology of *Orchis spectabilis* (L.) (Orchidaceae). *Ohio Journal of Science*, **82**: 218–225.

DODD, C.K. 1981. Infrared reflectance in chameleons (Chameleonidae) from Kenya. *Biotropica*, **13**: 161–164.

EMERSON, S.B., COOPER, T.A. & EHLERINGER, J.R. 1990. Convergence in reflectance spectra among treefrogs. *Functional Ecology*, **4**: 47–51.

EMMERTON, J. & DELHIS, J.D. 1980. Wavelength discrimination in the 'visible' and ultraviolet spectrum by pigeons. *Journal of Comparative Physiology*, **141**: 47–52.

FURE, A. 2006. Bats and lighting. *London Naturalist*, **85**: 1–20.

GAUTIER, C., O'HIROK, W. & RICCHIAZZI, P. 1999. Spectral signature of solar radiation absorption. Ninth Atmospheric Radiation Measurement Science Team Meeting Proceedings, 1–7. Albuquerque, NM, USA.

GIOKAS, S., PAFILIS, P. & VALAKOS, E. 2005. Ecological and physiological adaptations of the land snail *Albinaria caerulea* (Pulmonata: Clausiliidae). *Journal of Molluscan Studies*, **71**: 15–23.

GODFREY, D., LYTHGOE, J.N. & RUMBALL, D.A. 1987. Zebra stripes and tiger stripes: the spatial frequency distribution of the pattern compared to that of the background is significant in display and crypsis. *Biological Journal of the Linnean Society*, **32**: 427–433.

GRANT, R.H., HEISLER, G.M., GAO, W. & JENKS, M. 2003. Ultraviolet leaf reflectance of common urban trees and the prediction of reflectance from leaf surface characteristics. *Agricultural and Forest Meteorology*, **120**: 127–139.

HEATH, D.J. 1975. Colour, sunlight and internal temperatures in the land-snail *Cepaea nemoralis* (L.). *Oecologia*, **19**: 29–38.

HECHT, S. & PIRENNE, M.H. 1940. The sensibility of the nocturnal long-eared owl in the spectrum. *Journal of General Physiology*, **23**: 709–717.

HEDEGAARD, C., BARDEAU, J.-F. & CHATEIGNER, D. 2006. Molluscan shell pigments: an *in situ* resonance Raman study. *Journal of Molluscan Studies*, **72**: 157–162.

HELLER, J. & VOLOKITA, M. 1981. Shell banding polymorphism of the land snail *Xeropicta vestalis* along the coastal plain of Israel. *Biological Journal of the Linnean Society*, **16**: 279–284.

HEPPNER, J.B. 2008. Butterflies and moths. In: *Encyclopedia of entomology*. Edn 2. (J.L. Capinera, ed.), pp. 626–672.

HOCKING, B. & MITCHELL, B.L. 2008. Owl vision. *Ibis*, **103a**: 284–288.

HORRIDGE, G.A. 2009. *What does the honeybee see, and how do we know? A critique of scientific reasoning*. Australian National University E-Press.

HUNT, S., CUTHILL, I.C., SWADDLE, J.P. & BENNETT, A.T.D. 1997. Ultraviolet vision and band-colour preferences in female zebra finches, *Taeniopygia guttata*. *Animal Behaviour*, **54**: 1383–1392.

IMAFUKU, M., HIROSE, Y. & TAKEUCHI, T. 2002. Wing colors of *Chrysozephyrus* butterflies (Lepidoptera; Lycaenidae): ultraviolet reflection by males. *Zoological Science*, **19**: 175–83.

JACOBS, G.H., NEITZ, J. & DEEGAN, J.F. 1991. Retinal receptors in rodents maximally sensitive to ultraviolet light. *Nature*, **353**: 655–656.

JAMESON, K.A., HIGHNOTE, S.M. & WASSERMAN, L.M. 2001. Richer color experience in observers with multiple photopigment opsin genes. *Psychonomic Bulletin and Review*, **8**: 244–261.

JONES, J.S. 1982. Genetic differences in individual behaviour associated with shell polymorphism in the snail *Cepaea nemoralis*. *Nature*, **298**: 749–750.

KING, T. 2005. Human color perception, cognition and culture: Why 'red' is always red. *Imaging Science & Technology Reporter*, **20**: 1–7.

KOMAREK, S. 1998. *Mimicry, aposematism and related phenomena in animals and plants*. Vesmir, Prague, Czech Republic.

KREITHEN, M.L. & EISNER, T. 1978. Detection of ultraviolet light by the homing pigeon. *Nature*, **272**: 347–348.

LALL, A.B. & CRONIN, T.W. 1987. Spectral sensitivity of the compound eyes in the purple land crab *Gecarcinus lateralis* (Freminville). *Biological Bulletin*, **173**: 398–406.

LEONARD, A.S. & PAPAJ, D.R. 2011. 'X' marks the spot: the possible benefits of nectar guides to bees and plants. *Functional Ecology*, **25**: 1293–1301.

LIM, M.L.M. & LI, D. 2006. Extreme ultraviolet sexual dimorphism in jumping spiders (Araneae: Salticidae). *Biological Journal of the Linnean Society*, **89**: 397–406.

LUO, D.-G., YUE, W.W.S., ALA-LAURILA, P. & YAU, K.-W. 2011. Activation of visual pigments by light and heat. *Science*, **332**: 1307–1312.

LYYTINEN, A., LINDSTRÖM, L. & MAPPES, J. 2004. Ultraviolet reflection and predation risk in diurnal and nocturnal Lepidoptera. *Behavioral Ecology*, **15**: 982–987.

MARTIN, G.R. 1986. Sensory capacities and the nocturnal habits of owls (Strigiformes). *Ibis*, **128**: 266–277.

MEDEL, R., BOTTO-MAHAN, C. & KALIN-ARROYO, M. 2003. Pollinator-mediated selection on the nectar guide phenotype in the Andean monkey flower, *Mimulus luteus*. *Ecology*, **84**: 1721–1732.

MEINHARDT, H. 2009. *The algorithmic beauty of sea shells*. Edn 4. Springer, Berlin, Germany.

MORENO-RUEDA, G. 2007. Refuge selection by two sympatric species of arid-dwelling land snails: Different adaptive strategies to achieve the same objective. *Journal of Arid Environments*, **68**: 588–598.

MORENO-RUEDA, G. 2008. The color white diminishes weight loss during aestivation in the arid-dwelling land snail *Sphincterochila (Albea) candidissima*. *Iberus*, **26**: 47–51.

MÜLLER, B., GLÖSMANN, M., PEICHL, L., KNOP, G.C., HAGEMANN, C. & AMMERMÜLLER, J. 2009. Bat eyes have ultraviolet-sensitive cone photoreceptors. *PLoS One*, **4**: e6390. doi:10.1371/journal.pone.0006390.

MURPHY, M.J. 2002. Observations on the behavior of the Australian land snail *Hedleyella falconeri* (Gray, 1834) (Pulmonata: Caryodidae) using the spool-and-line tracking technique. *Molluscan Research*, **22**: 149–164.

MURRAY, E. 1998. Distribution and status of native carnivorous land snails in the genera *Wainuia* and *Rhytida*. *Science for Conservation*, **101**: 1–49.

NEWBOLD, H.G. & KING, C.M. 2009. Can a predator see 'invisible' light? Infrared vision in ferrets (*Mustela furo*). *Wildlife Research*, **36**: 309–318.

ÖDEEN, A., HÅSTAD, O. & ALSTRÖM, P. 2011. Evolution of ultraviolet vision in the largest avian radiation—the passerines. *BMC Evolutionary Biology*, **11–313**: 1–8. doi:10.1186/1471-2148-11-313.

PAYNE, R.S. 1971. Acoustic location of prey by barn owls (*Tyto alba*). *Journal of Experimental Biology*, **54**: 535–573.

PEICHL, L., CHAVEZ, A.E., OCAMPO, A., MENA, W., BOZINOVIC, F. & PALACIOS, A.G. 2005. Eye and vision in the subterranean rodent cururo (*Spalacopus cyanus*, Octodontidae). *Journal of Comparative Neurology*, **486**: 197–208.

POMEROY, D.E. 1968. Dormancy in the land snail, *Helicella virgata* (Pulmonata: Helicidae). *Australian Journal of Zoology*, **16**: 857–869.

PRIMACK, R.B. 1982. Ultraviolet patterns in flowers, or flowers as viewed by insects. *Arnoldia*, **42**: 139–146.

RICHARDSON, A.M.M. 1974. Differential climatic selection in natural population of land snail *Cepaea nemoralis*. *Nature*, **247**: 572–573.

ROSIN, Z.M., OLBORSKA, P., SURMACKI, A. & TRYJANOWSKI, P. 2011. Differences in predatory pressure on terrestrial snails by birds and mammals. *Journal of Bioscience*, **36**: 691–699.

ROWE, C., (ed.) 2001. Warning signals and mimicry. *Evolutionary Ecology*, **13**: 601–827.

RUTOWSKI, R.L. & MACEDONIA, J.M. 2008. Limits on the wavelengths represented in ultraviolet images of Lepidoptera. *Journal of the Lepidopterists' Society*, **62**: 133–137.

16

SAVAZZI, E. 2011. *Digital photography for science*. Lulu Press, Raleigh, NC, USA.

SCHEIL, A.E., KOHLER, H.R. & TRIEBSKORN, R. 2011. Heat tolerance and recovery in Mediterranean land snails after pre-exposure in the field. *Journal of Molluscan Studies*, **77**: 1–10.

SCHMIDT-NIELSEN, K., TAYLOR, C.R. & SHKOLNIK, A. 1971. Desert snails: problems of heat, water and food. *Journal of Experimental Biology*, **55**: 385–398.

SEILACHER, A. 1972. Divaricate patterns in pelecypod shells. *Lethaia*, **5**: 325–343.

SHAW, G.A., SIEGEL, A.M., MODEL, J., GEBOFF, A., SOLOVIEV, S., VERT, A. & SANDVIK, P. 2009. Deep UV photon-counting detectors and applications. *Proceedings of the Society of Photo-optical Instrumentation Engineers*, **7320**: 73200J-2, doi: 10.1117/12.820825.

SKELHORN, J., ROWLAND, H.M., SPEED, M.P. & RUXTON, G.D. 2010. Masquerade: Camouflage without crypsis. *Science*, **327**: 51.

SKELHORN, J. & RUXTON, G.D. 2010. Predators are less likely to misclassify masquerading prey when their models are present. *Biology Letters*, **6**: 597–599.

SKELHORN, J. & RUXTON, G.D. 2011. Mimicking multiple models: polyphenetic masqueraders gain additional benefits from crypsis. *Behavioral Ecology*, **22**: 60–65.

SLOTOW, R., GOODFRIEND, W. & WARD, D. 1993. Shell colour polymorphism of the Negev desert landsnail, *Trochoidea seetzeni*: the importance of temperature and predation. *Journal of Arid Environments*, **24**: 47–61.

SLOTOW, R. & WARD, D. 1997. Habitat constraints on shell-colour variation of a desert landsnail, *Trochoidea simulata*. *Journal of Molluscan Studies*, **63**: 197–205.

STARR, C. 2005. *Biology: concepts and applications*. Thomson Brooks—Cole, Belmont, CA, USA.

STEVENS, M. & MERILAITA, S. 2011a. Crypsis through background matching. In: *Animal camouflage; mechanisms and function* (M. Stevens & S. Merilaita, eds), pp. 17–33.

STEVENS, M. & MERILAITA, S. 2011b. Animal camouflage; function and mechanisms. *Animal camouflage; mechanisms and function* (M. Stevens & S. Merilaita, eds.), pp. 1–16.

TILLEY, J.D. 2011. *Colour and the optical properties of materials*. Wiley & Sons, Chichester, UK.

TROSCIANKO, T., BENTON, C.P., LOVELL, B.P., TOLHURST, D.J. & PIZLO, Z. 2011. Camouflage and visual perception. In: *Animal camouflage; mechanisms and function* (M. Stevens & S. Merilaita, eds), pp. 118–144.

TURNER, J.S. & LOMBARD, A.T. 1990. Body colour and body temperature in white and black Namib desert beetles. *Journal of Arid Environments*, **19**: 305–315.

UGOLINI, A., BORGIOLI, G., GALANTI, G., MERCATELLI, L. & HARIYAMA, T. 2010. Photoresponses of the compound eye of the sandhopper *Talitrus saltator* (Crustacea, Amphipoda) in the ultraviolet-blue range. *Biological Bulletin*, **219**: 72–79.

VANDERPLANK, F.-L. 1934. The effect of infra-red waves on tawny owls (*Strix aluco*). *Proceedings of the Zoological Society of London*, **1934**: 505–507.

VERHOEVEN, G.J. 2008. Imaging the invisible using modified digital still cameras for straightforward and low-cost archaeological near-infrared photography. *Journal of Archaeological Science*, **35**: 3087–3100.

VERHOEVEN, G.J. & SCHMITT, K.D. 2008. An attempt to push back frontiers—digital near-ultraviolet aerial archaeology. *Journal of Archaeological Science*, **37**: 833–845.

VERHOEVEN, G.J., SMET, P., POELMAN, D. & VERMEULEN, F. 2009. Spectral characterisation of a digital still camera's NIR-modification to enhance archaeological observation. *IEEE Transactions on Geoscience and Remote Sensing*, **47**: 3456–3468.

WARD, J.M., BLOUNT, J.D., RUXTON, G.D. & HOUSTON, D.C. 2002. The adaptive significance of dark plumage for birds in desert environments. *Ardea*, **90**: 311–323.

WILLIAMS, G.A., CALDERONE, J.B. & JACOBS, G.H. 2005. Photoreceptors and photopigments in a subterranean rodent, the pocket gopher (*Thomomys bottae*). *Journal of Comparative Physiology A, Neuroethology, Sensory, Neural and Behavioral Physiology*, **191**: 125–134.

WINTER, Y., LÓPEZ, J. & VON HELVERSON, O. 2003. Ultraviolet vision in a bat. *Nature*, **425**: 612–614.

WOODBRIDGE, R.G. 1961. *Fluorescent shells: a monograph on fluorescent mollusk shells of the seas, the shores, the freshwaters and the lands of the world*. Transspace Laboratory, Trenton, NJ, USA.

YAMAMOTO, G. 1962. Direct absorption of solar radiation by atmospheric water vapor, carbon dioxide and molecular oxygen. *Journal of the Atmospheric Sciences*, **19**: 182–188.

YOKOYAMA, S. & SHI, Y. 2000. Genetics and evolution of ultraviolet vision in vertebrates. *Federation of European Biochemical Societies (FEBS) Letters*, **486**: 167–172.

YORK, W., LÓPEZ, J. & VON HELVERSON, O. 2003. Ultraviolet vision in a long-tongued nectar bat (*Glossophaga soricina*). *Nature*, **425**: 612–614.

YOSHIMURA, H., ZHU, H., WU, Y. & MA, R. 2010. Spectral properties of plant leaves pertaining to urban landscape design of broad-spectrum solar ultraviolet radiation reduction. *International Journal of Biometeorology*, **54**: 179–91.